



RESEARCH MEMORANDUM

NOTES ON A LARGE-SCALE STATISTICAL PROGRAM FOR THE
ESTABLISHMENT OF MANEUVER-LOADS DESIGN CRITERIA
FOR MILITARY AIRPLANES

By John P. Mayer, Ralph W. Stone, Jr.,
and Harold A. Hamer

Langley Aeronautical Laboratory
Langley Field, Va.

NATIONAL ADVISORY COMMITTEE
FOR AERONAUTICS
WASHINGTON

July 17, 1957
Declassified February 26, 1958

THIS PAGE IS UNCLASSIFIED

ERRATA

NACA Research Memorandum L57E30

By John P. Mayer, Ralph W. Stone, Jr., and Harold A. Hamer
July 1957

Page 2: Correct definitions for first three symbols under "Symbols and Coefficients" as follows:

a_x longitudinal acceleration (positive forward), ft/sec²

a_y lateral acceleration (positive to right of plane of symmetry),
ft/sec²

a_z normal acceleration (positive below XY body plane), ft/sec²

Page 3: Correct definitions of last three symbols on page as follows:

L_x longitudinal aerodynamic load (positive forward), lb

L_y lateral aerodynamic load (positive to right of plane of
symmetry), lb

L_z normal aerodynamic load (positive above XY body plane), lb

Page 12: The third equation of equations (2) should read

$$L_{Z,A} = - \frac{W}{g} a_{Z,cg}$$

(Continued on next page)

THIS PAGE IS UNCLASSIFIED

Issued 10/4/57

THIS PAGE IS UNCLASSIFIED

Page 17: The first and second equations of equations (9a) should read

$$L_{Z,H} = \frac{I_Y}{x_{t,H}} \dot{q} - \frac{(I_Z - I_X)}{x_{t,H}} pr - \frac{I_{XZ}}{x_{t,H}}(r^2 - p^2) + \frac{I_{X,e}}{x_{t,H}} \omega_e r -$$

$$\frac{(C_{m,WF})_O S \bar{c}}{x_{t,H}} q_d + \frac{W \bar{c}}{g(x_{t,H})} \left[\frac{C_{m,WF} - (C_{m,WF})_O}{C_{N,WF}} \right] a_{Z,cg}$$

$$L_{Z,WF} = - \frac{W x_H}{g(x_{t,H})} a_{Z,cg} - \frac{I_Y}{x_{t,H}} \dot{q} + \frac{(I_Z - I_X)}{x_{t,H}} pr + \frac{I_{XZ}}{x_{t,H}}(r^2 - p^2) -$$

$$\frac{I_{X,e}}{x_{t,H}} \omega_e r + \frac{(C_{m,WF})_O S \bar{c}}{x_{t,H}} q_d$$

THIS PAGE IS UNCLASSIFIED

NATIONAL ADVISORY COMMITTEE FOR AERONAUTICS

RESEARCH MEMORANDUM

NOTES ON A LARGE-SCALE STATISTICAL PROGRAM FOR THE
ESTABLISHMENT OF MANEUVER-LOADS DESIGN CRITERIA
FOR MILITARY AIRPLANES

By John P. Mayer, Ralph W. Stone, Jr.,
and Harold A. Hamer

SUMMARY

An outline is presented of a statistical program to collect data for the establishment of more realistic maneuver-loads design criteria. Some details on the loads derivable from the measured quantities and the accuracy with which these loads may be obtained are discussed. In addition, some sample experimental data are used to indicate possible methods of statistical analysis for the assessment of maneuver-loads criteria and some remarks are made on the sample size required for the overall program. The methods used and the results possible from such a statistical program represent a goal which could be obtained under the assumptions made; however, many of the operations indicated in the outline for the statistical analysis are not known and will require further study. An actual program may differ in many respects to that presented, such differences depending in part upon the type and accuracy of the recording instrument selected.

INTRODUCTION

Present maneuver-loads design criteria have been established, where possible, on the basis of past experience. In some instances, however, past experience is either inadequate or unavailable in which case it has been necessary to resort to the specification of arbitrary factors and conditions in the maneuver-loads criteria. In recent years the effect of size and performance on the structural weight of aircraft has put increased emphasis on the design criteria and statistical verification of the existing criteria appears to be desirable.

In order to obtain this statistical verification of design load criteria, the military services have in the past used V-G and VGH recorders to measure airspeed, altitude, and normal load factor; however, in order

to assess properly the design load criteria, it was evident that the number of measured parameters should be increased. After an assessment of the problem, a special panel of the NACA Subcommittee on Aircraft Loads recommended that the statistical loads programs be expanded to measure time histories of eight parameters (the three linear accelerations, the three angular accelerations, airspeed, and altitude) and that a study be made covering utilization of the data in relation to design criteria, analysis techniques, and the required sample size.

The National Advisory Committee for Aeronautics is presently engaged in assisting the U. S. Air Force and the Bureau of Aeronautics (Department of the Navy) in a cooperative program aimed at the expansion of the maneuver-loads statistical programs and development of methods for utilizing the statistical data in the design criteria. The present report is concerned with some preliminary results in connection with the study phase of the program and presents an outline of a suggested statistical program. In addition, some comments are made about the component loads that may be derived from the measured quantities and the accuracy with which these loads may be obtained. Some sample experimental data are used to indicate possible methods of statistical analysis for the assessment of maneuver-loads criteria and, finally, a brief study of the sample size required for the overall program is presented.

In addition, this paper indicates some of the methods that could be used and some of the results possible from such a statistical program and represents a goal which could be attained under the assumptions made. An actual program may differ in many respects from that presented herein, such differences depending in part upon the type and accuracy of the recording instrument selected.

SYMBOLS AND COEFFICIENTS

The body system of axes has been used in this analysis and the forces, moments, loads, and airplane motions are referred to these axes:

a_x	longitudinal acceleration, ft/sec ²
a_y	lateral acceleration, ft/sec ²
a_z	normal acceleration, ft/sec ²
b	wing span, ft
\bar{c}	mean aerodynamic chord, ft

C_m	pitching-moment coefficient, $M_Y/q_d S \bar{c}$
C_N	normal-force coefficient, $n_Z W/q_d S$
C_n	yawing-moment coefficient, $M_Z/q_d S b$
C_Y	lateral-force coefficient, $n_Y W/q_d S$
$\frac{\partial C_m}{\partial C_N}$	rate of change of pitching-moment coefficient with normal-force coefficient
$\frac{\partial C_n}{\partial C_Y}$	rate of change of yawing-moment coefficient with lateral-force coefficient
$f\{y\}$	probability density function of y
f_W, f_H, f_V	probability of occurrence of a component load
$f_{1,P2}; f_{2,P2}; f_{1,1-P1}; f_{2,1-P1}$	factors used in determining confidence curves
g	acceleration due to gravity, 32.2 ft/sec ²
h	altitude, ft
I_X	moment of inertia about X body axis, slug-ft ²
I_Y	moment of inertia about Y body axis, slug-ft ²
I_Z	moment of inertia about Z body axis, slug-ft ²
I_{XZ}	product of inertia (positive when principal axis is inclined below X body axis), slug-ft ²
$I_{X,e}$	moment of inertia of rotating engine parts about X body axis, slug-ft ²
L_X	longitudinal aerodynamic load, lb
L_Y	lateral aerodynamic load, lb
L_Z	normal aerodynamic load, lb

M	Mach number
M_X	aerodynamic rolling moment, ft-lb
M_Y	aerodynamic pitching moment, ft-lb
M_Z	aerodynamic yawing moment, ft-lb
N	total number of observations
n_X	longitudinal load factor, $a_{X,cg}/g$
n_Y	lateral load factor, $a_{Y,cg}/g$
n_Z	normal load factor, $-a_{Z,cg}/g$
p	rolling velocity, radians/sec
\dot{p}	rolling acceleration, radians/sec ²
p_h	static pressure, lb/sq ft
$P\{y\}; p(y)$	probability that a given value y will occur
$P(y)$	probability of exceeding a given value y
P'	probability limits associated with confidence curves
q	pitching velocity, radians/sec
\dot{q}	pitching acceleration, radians/sec ²
q_c	impact pressure, lb/sq ft
q_d	dynamic pressure, lb/sq ft
r	yawing velocity, radians/sec
\dot{r}	yawing acceleration, radians/sec ²
S	wing area, sq ft
T	total flight time

V	true airspeed, ft/sec
$v_{P_2}^2, v_{1-P_1}^2$	variance ratios used in confidence curves
W	airplane weight, lb
$x_{t,H}$	distance between aerodynamic center of wing-fuselage combination (in pitch plane) and aerodynamic center of horizontal tail parallel to X body axis, $x_H - x_{Z,WF}$, ft
$x_{t,V}$	distance between aerodynamic center of wing-fuselage combination (in yaw plane) and aerodynamic center of vertical tail parallel to X body axis, $x_V - x_{Y,WF}$, ft
x_H	longitudinal distance between aerodynamic center of horizontal tail and center of gravity parallel to X body axis (negative for tail behind center of gravity), ft
x_V	longitudinal distance between aerodynamic center of vertical tail and center of gravity parallel to X body axis (negative for tail behind center of gravity), ft
z_V	normal distance between aerodynamic center of vertical tail and center of gravity parallel to Z body axis (negative for tail above X body axis), ft
$x_{Y,WF}$	distance between aerodynamic center of wing-fuselage combination (in yaw plane) and center of gravity parallel to X body axis (positive when forward of center of gravity), ft
$x_{Z,WF}$	distance between aerodynamic center of wing-fuselage combination (in pitch plane) and center of gravity parallel to X body axis (positive when forward of center of gravity), ft
x_a	longitudinal distance of accelerometer from center of gravity parallel to X body axis, ft
y_a	lateral distance of accelerometer from center of gravity parallel to Y body axis, ft
z_a	normal distance of accelerometer from center of gravity parallel to Z body axis, ft
ϵ	maximum error, lb

σ	root-mean-square error (assumed to be $\epsilon/3$), lb
σ_y	standard deviation of y (root mean square)
ω_e	engine rotational velocity, radians/sec

Subscripts:

O	zero lift
A	total airplane
bal	balancing
cg	center of gravity
F	fuselage
H	horizontal tail
L	left
lim	limit load
man	maneuvering
meas	measured
opt	optimum
R	right
V	vertical tail
W	wing
WF	wing fuselage

OUTLINE OF A STATISTICAL MANEUVER-LOADS PROGRAM

Some statistical studies applicable to maneuver-loads design criteria have been made in the past, such as, for example, those reported in references 1, 2, and 3. Such studies, however, are applicable only to specific regions of the design problem. The subject of statistical loads research, therefore, was examined to determine an integrated approach to the overall problem on the basis of the eight measured quantities

previously mentioned. This approach is presented herein as a possible outline for assessing maneuver-loads design criteria. The tentative outline for the complete program is presented in figure 1 as a block diagram. The program can be considered in three parts: (1) the data recording phase, (2) the basic data reduction and computing phase, and (3) the data analysis and design criterion phase. It must be admitted that, at this time, the operations involved in some of the blocks within each phase are not known.

Data-Recording Phase and Measured Quantities

It will be assumed that the quantities that will be measured are: impact pressure, q_c ; static pressure, p_h ; longitudinal acceleration, a_x ; lateral acceleration, a_y ; normal acceleration, a_z ; rolling velocity, p ; pitching velocity, q ; and yawing velocity, r . (It should be noted that, at this time, there is a question of whether the quantities measured should be angular velocities p , q , and r or angular accelerations \dot{p} , \dot{q} , and \dot{r} . It is believed that it might be preferable to measure the angular velocities and differentiate them at the recorder or in the playback equipment. This is mostly a question of instrument accuracy. If an angular accelerometer could be made as accurate as an angular velocity recorder, the accelerometer might be preferred since integration is ordinarily a more accurate operation than differentiation; however, if the accelerometer is not accurate, large errors can build up in the integrating process in a short time, in which case the differentiation of angular velocity might prove to be preferable. This is an important question and must be given careful consideration.) The impact pressure q_c and the static pressure p_h are the basic measurements from which Mach number, altitude, and airspeed are derived.

Since it will be unlikely that the linear accelerometers can be placed exactly at the center of gravity, some provisions must be made to transfer the measured results to the airplane center of gravity. By means of the following transformations, the true accelerations at the center of gravity are given in terms of the measured accelerations as:

$$\left. \begin{aligned} a_{X,cg} &= a_{X,meas} + x_a(q^2 + r^2) + y_a(\dot{r} - pq) - z_a(\dot{q} + rp) \\ a_{Y,cg} &= a_{Y,meas} + y_a(r^2 + p^2) + z_a(\dot{p} - qr) - x_a(\dot{r} + pq) \\ a_{Z,cg} &= a_{Z,meas} + z_a(p^2 + q^2) + x_a(\dot{q} - rp) - y_a(\dot{p} + qr) \end{aligned} \right\} \quad (1)$$

It is seen from equations 1 that both the angular velocities and angular accelerations must be known in order to obtain the corrected linear accelerations.

The corrections to the measured transverse accelerations are extremely important especially for fighter airplanes where accelerometer locations as little as 1 foot from the center of gravity in the Y- or Z-direction result in errors often larger than the true value of the acceleration.

Basic Data Reduction

It would be desirable if the output of the recording system could be fed into a computing facility so that the statistical parameters of basic interest, which are discussed in later sections, could be obtained in one continuous operation. The basic operations are indicated in the blocks numbered 3 to 7 and other possible operations are indicated in blocks numbered 19 to 25 of figure 1.

Data editing.- The first step in the data reduction would be an editing process (block 3, fig. 1). Certain historical information would have to be retained such as recorder number, airplane type and number, flight number, airplane configuration, and so forth. Certainly all the flight time will not be in maneuvering flight or in rough air. Therefore, the first step in the editing process would be to filter out all the smooth - nonmaneuvering flight. It is expected that this editing could be accomplished by using a specified magnitude of a given quantity as a threshold below which the data could be deleted. Of course, the flight time represented by the deleted data would be saved.

The next step in the editing process would be to separate maneuvers from gusts. This would be a difficult operation and probably could be accomplished by using the frequency characteristics of the airspeed or load factor fluctuations as a guide.

In the operations described above, it is not implied that all the editing processes should be performed in one editing device. It might be preferable to separate the operations.

Computing phase.- The basic edited output in figure 1 in block number 4 would consist of the eight measured quantities p_h , q_c , $a_{x,meas}$, $a_{z,meas}$, $a_{y,meas}$, p , q , and r . Certain basic computations (block 5) would have to be made such as converting the input into the correct dimensional form for the various quantities; calculating airspeed, altitude, Mach number, and dynamic pressure; integrating the angular accelerations (or differentiating the angular velocities); and calculating the center-of-gravity linear accelerations (eqs. (1)) from the measured accelerations.

The output of the computing phase (block 6) might consist of the following components which are considered to be pertinent to the loads on an airplane and thus desirable to examine in a statistical manner:

$$\begin{array}{ll}
 V = f(p_h, q_c) & q_r \\
 h = f(p_h) & p_r \\
 M = f(p_h, q_c) & \dot{r} + pq \\
 & \dot{p} - qr \\
 & r^2 - p^2 \\
 q_d & \\
 \dot{p} = dp/dt & \\
 \dot{q} = dq/dt & \left. \begin{array}{l} a_{X, cg} \\ a_{Y, cg} \\ a_{Z, cg} \end{array} \right\} \text{from equations 1} \\
 \dot{r} = dr/dt & \\
 pq &
 \end{array}$$

It is evident that maximum use must be made of automatic data-handling equipment and computers to handle the large amount of statistical data expected in a large-scale program.

Statistical data reduction (blocks 7 and 8, fig. 1).— The statistical data reduction would yield probability distributions and envelopes of maximum values. The probability distributions would be in three forms: (1) peak distributions of each quantity showing probability of exceeding given peak values, (2) time distributions showing time spent above a given value, and (3) time-to-exceed distributions showing average time required to exceed a given peak value. These distributions might be in the form of correlation tables with airspeed and altitude as parameters. In addition to the probability distributions for individual and combined quantities, some cross correlations will be necessary.

In the process of computing the peak counts for the probability distributions, the data would be in a form to obtain envelope plots. The envelopes would consist of plots of the maximum values of any quantity against airspeed, Mach number, or another quantity. The envelopes could be used for comparison with the known capabilities of the airplanes and the design criteria.

In the statistical data-reduction phase, one of the important questions is the method of counting peak values. There are many ways of counting peak values, and the method chosen should be compatible with the use to which the peak values are to be put, such as in fatigue, maximum loads, and so forth. Some peak counting methods are given in references 4 to 6.

Other operations.- In figure 1, other operations (blocks 19 to 25) are shown within the computing facility block. The operations shown are the calculation of component loads from the basic parameters and the harmonic analysis of the data. At this time this group of operations are considered subordinate to the main line of operations shown as blocks 3 to 7 in figure 1. Nevertheless, it might be desirable to calculate the component-load probability distributions in some cases as indicated in figure 1. More will be said about the calculation of loads in another section of this paper.

In the harmonic analysis (block 25), use could be made of power-spectral-analysis methods for both gusts and maneuvers. The value of spectral analyses in evaluating gust data is fairly well understood; however, the use of these methods for maneuvers is open to question. There is evidence, however, that such methods may prove valuable, at least for determining the frequency content of control inputs and airplane responses. (See refs. 5 and 7 for example.) These results will be useful in the design of automatic or power control systems.

Data Analysis and Design Criteria

The output of the computing facility (block 8, fig. 1) consisting of correlation tables, probability curves, and envelope curves will be the information from which the design criteria and design loads for future aircraft may be obtained. An indication of the possible steps involved are indicated in blocks numbered 9 to 18 of figure 1. As stated previously, some of the details of the operations in blocks 9 to 18 are not well known. Although considerably more work needs to be done along these lines, some thought has been given to these problems and some results have been obtained.

One of the important tasks will be the transformation of information obtained on the test airplanes into more generalized information (block 9). The job here will be to attempt to separate out the individual airplane characteristics and the effect of specific missions.

The effect of specific missions probably could be obtained by sorting the data by mission type. At this stage it would be most important to check the validity of calculated probability curves for specific missions with the experimental curves. (See refs. 1 and 3 for example.)

In order to separate out individual airplane characteristics such as those associated with stability differences, it may be possible to standardize or normalize the probability curves for airplanes of a general category, for example, interceptors. This standardization would give a probability curve for each of the airplane categories and comparison of airplanes in the same category would be facilitated. To remove

the effect of the individual airplane characteristics would be a rather difficult and complex operation. One possible way to accomplish this operation might be to divide the amplitude ratios of the frequency response of the different airplanes by a standard amplitude ratio. At the present time, the statistical data available are not sufficient to prove or disprove this suggestion, partly because the transfer functions of the airplanes for which data are available are not different enough from each other and partly because the statistical reliability of the data is not good enough to show the differences.

The results of this standardization process appear in block 10 and are called "statistical parameters of existing airplanes" to distinguish them from results in block 8 which are the specific statistical parameters of the test airplanes. Of the two cases, it is believed that the standardized form of statistical information is more amenable for use in developing maneuver-loads design criteria and for determining the design loads of prospective airplanes. In figure 1 these developments are indicated by blocks 11 to 12 and 13 to 18. When the statistical parameters for obtaining design loads of a prospective airplane (block 14) are determined, the new airplane characteristics and new mission effects would first have to be accounted for. Next, from these statistical parameters which are the probability curves for the basic quantities, the probability curves for the component airplane loads may be determined by using the equations of motion and the mass characteristics of the proposed airplane (block 16). These load-probability curves could be used for determining the design loads. It is probable that the optimum design loads for the various airplane components are a function of the probability curves for all the components (blocks 17 and 18). If, for example, the wing and tail were designed for equal probability of failure, the probability of either a wing or a tail failure might be much higher. This effect is discussed in a subsequent section of this paper.

Although the statistical parameters are useful for determining airplane design loads, these loads can not be determined without the careful interpretation of the methods in which the statistical results are to be used through the design load criteria (blocks 11 and 12). For example, the airplane procuring services might specify, among other things, the probability level which will be acceptable for design and the specific-mission effects for which the probability curves might be adjusted.

As was noted previously, the operations indicated in many of the blocks shown in figure 1 are not known at this time; however, some progress has been made in defining the operations. The remaining sections of this paper will deal with some of the results obtained.

LOADS DERIVABLE FROM MEASURED QUANTITIES

The purpose of the statistical loads program, as has been noted previously, is to rationalize maneuver-loads criteria so that new airplane configurations may be designed more realistically than is now possible. In order to accomplish this purpose, as is noted in figure 1, it appears desirable to derive the loads that may be encountered on a new configuration from the probability distributions of the motions that this airplane may encounter. This derivation may be made through the probability distributions of these motions, which can be obtained by transforming the motions measured on existing operational airplanes (fig. 1) and by a knowledge of the geometric, aerodynamic, and mass parameters which relate these motions to the loads.

In order to maintain a check on the statistical methods developed for the design criteria as well as to monitor the loads being obtained it may also be desirable in some cases (as noted in fig. 1, blocks 19 to 21 and 26 to 29) to determine the probability distributions of the loads that were encountered on the operational airplane used in making the measurements. This may be accomplished through the probability distributions of the motions encountered and the parameters relating these motions to the loads or through the basic measurements and these parameters. In either event, an evaluation of the various geometric, aerodynamic, and mass parameters would be required. The equations of motion of the airplane and the equations of the summation of loads acting on the airplane would also be required to establish these parameters and the relation of the loads to the motions encountered.

The total aerodynamic loads and moments acting on an airplane are related to the measured quantities through the equations of motion as follows:

$$\left. \begin{aligned}
 I_{X,A} &= \frac{W}{g} a_{X,cg} \\
 I_{Y,A} &= \frac{W}{g} a_{Y,cg} \\
 I_{Z,A} &= \frac{W}{g} a_{Z,cg} \\
 M_X &= I_X \dot{p} - (I_Y - I_Z)qr - I_{XZ}(\dot{r} + pq) \\
 M_Y &= I_Y \dot{q} - (I_Z - I_X)pr - I_{XZ}(r^2 - p^2) + (I_{X,e})\omega_e r \\
 M_Z &= I_Z \dot{r} - (I_X - I_Y)pq - I_{XZ}(\dot{p} - qr) - (I_{X,e})\omega_e q
 \end{aligned} \right\} \quad (2)$$

The total airplane loads ($L_{X,A}$, $L_{Y,A}$, and $L_{Z,A}$) and airplane moments (M_X , M_Y , and M_Z) are thus directly derivable from the measured quantities and the derived angular accelerations if the airplane weight and inertia characteristics are known.

A breakdown of the total loads into loads on the various parts of the airplane, such as the wing and tail surfaces, requires knowledge of other airplane characteristics. Such additional information must be obtained from complete flight tests of the airplane or from wind-tunnel tests of models of the particular configuration. If the airplane were divided into its six major components (the fuselage, the right- and left-wing panels, the right and left horizontal-tail panels, and the vertical tail (see fig. 2)), loads would act on each of these components in such a way that their sums would be equal to the total loads and the moments created would be equal to the total moments. Equations expressing this relation are:

$$\left. \begin{aligned} L_{X,A} &= L_{X,F} + L_{X,WR} + L_{X,WL} + L_{X,HR} + L_{X,HL} + L_{X,V} \\ L_{Y,A} &= L_{Y,F} + L_{Y,WR} + L_{Y,WL} + L_{Y,HR} + L_{Y,HL} + L_{Y,V} \\ L_{Z,A} &= L_{Z,F} + L_{Z,WR} + L_{Z,WL} + L_{Z,HR} + L_{Z,HL} + L_{Z,V} \\ M_X &= M_{X,F} + M_{X,WR} + M_{X,WL} + M_{X,HR} + M_{X,HL} + M_{X,V} \\ M_Y &= M_{Y,F} + M_{Y,WR} + M_{Y,WL} + M_{Y,HR} + M_{Y,HL} + M_{Y,V} \\ M_Z &= M_{Z,F} + M_{Z,WR} + M_{Z,WL} + M_{Z,HR} + M_{Z,HL} + M_{Z,V} \end{aligned} \right\} \quad (3)$$

It is clearly evident that solution of equations (3) for the individual parts on the right-hand side of the equations is impossible from the measurements contemplated. Some simplifying concepts and additional information, however, may be introduced to reduce the problem for solution. Any of the three moments M_X , M_Y , and M_Z are affected by the two components of force acting perpendicular to the axis about which the particular moment acts. The lifting and stabilizing surfaces of an airplane create primarily Z- and Y-forces and are the primary contributors to all the moments acting on the airplane. From these comments and the fact that the X-force may frequently be nearly zero because of an equilibrium between thrust and drag, it would appear that the X-force and

its contribution to any moments could be neglected. If the thrust axis is removed from the center of gravity, however, further consideration of its effect must be made. A further simplification of the problem is obtained by combining certain components on the right-hand side of equations (3). In addition, certain terms in the equations, such as $L_{Z,V}$, $L_{Y,H}$, and $M_{Y,V}$, have negligible effect on the total forces and moments and may be neglected for most airplane types. If the horizontal tail has dihedral or if part of the vertical tail consists of skewed ventral fins, their contributions to the side force and yawing moment, and normal force and pitching moment, respectively, can not be neglected as is done here. With these simplifications, equations (3) are reduced to the following:

$$\left. \begin{aligned} L_{Y,A} &= L_{Y,WF} + L_{Y,V} \\ L_{Z,A} &= L_{Z,WF} + L_{Z,H} \\ M_X &= (M_{X,WF} + M_{X,H}) + M_{X,V} \\ M_Y &= M_{Y,WF} + M_{Y,H} \\ M_Z &= M_{Z,WF} + M_{Z,V} \end{aligned} \right\} \quad (4)$$

The moments may now be broken down into the forces or loads acting and the moment arms of these forces to axes through the center of gravity. It is most appropriate to do this with the tail contributions as these contributions can not cause couples about the center of gravity, and the moment arms to the tail aerodynamic centers may be estimated with reasonable accuracy. Thus,

$$\left. \begin{aligned} M_{X,V} &= -(L_{Y,V})z_V \\ M_{Y,H} &= (L_{Z,H})x_H \\ M_{Z,V} &= (L_{Y,V})x_V \end{aligned} \right\} \quad (5)$$

where the distances x_V , x_H , and z_V are estimated distances from the body axes to the respective tail aerodynamic centers. The distance z_V , being the shortest of these distances, would be estimated with the least accuracy; however, it appears in the rolling-moment equation where its contribution is generally small and may not significantly affect the results. Estimates of x_V and x_H for contemporary configurations could be made within 2 percent; however, increasing tail sizes or decreasing tail length will have the effect of increasing this error. The moments $M_{Y,WF}$ and $M_{Z,WF}$ also may be broken down in a similar manner, except for an effective couple about the center of gravity in the pitching moment.

$$\left. \begin{aligned} M_{Y,WF} &= (M_{Y,WF})_O + (L_{Z,WF})(x_{Z,WF}) \\ M_{Z,WF} &= (L_{Y,WF})(x_{Y,WF}) \end{aligned} \right\} \quad (6)$$

so that

$$\left. \begin{aligned} x_{Z,WF} &= \frac{M_{Y,WF} - (M_{Y,WF})_O}{L_{Z,WF}} = \left[\frac{C_{m,WF} - (C_{m,WF})_O}{C_{N,WF}} \right] \bar{c} \\ x_{Y,WF} &= \frac{M_{Z,WF}}{L_{Y,WF}} = \left(\frac{C_{n,WF}}{C_{Y,WF}} \right) b \\ (M_{Y,WF})_O &= (C_{m,WF})_O q_d S \bar{c} \end{aligned} \right\} \quad (7)$$

Values of $x_{Z,WF}$, $x_{Y,WF}$, and $(M_{Y,WF})_O$ may be determined only through a knowledge of the airplane characteristics. These characteristics must be obtained from complete wind-tunnel tests for prospective configurations and from wind-tunnel tests or flight tests of existing airplanes. The coefficients $C_{m,WF}$, $(C_{m,WF})_O$, $C_{N,WF}$, $C_{n,WF}$, and $C_{Y,WF}$ will likely be functions of Mach number, angle of attack, sideslip, and so forth;

consideration of this fact must be made in any given case. The accuracy of these coefficients depends on the accuracy of their measurement in flight or in wind-tunnel tests, and, if wind-tunnel values are used, the degree of correlation with flight values.

With the substitutions of the various factors just discussed (eqs. (5) and (6)), equations (4) become

$$\left. \begin{aligned} L_{Y,A} &= L_{Y,WF} + L_{Y,V} \\ L_{Z,A} &= L_{Z,WF} + L_{Z,H} \\ M_X &= M_{X,WF} + M_{X,H} - (L_{Y,V})z_V \\ M_Y &= (M_{Y,WF})_O + (L_{Z,WF})(x_{Z,WF}) + (L_{Z,H})x_H \\ M_Z &= (L_{Y,WF})(x_{Y,WF}) + (L_{Y,V})x_V \end{aligned} \right\} \quad (8)$$

These equations may now be solved for horizontal-tail load $L_{Z,H}$, the vertical-tail load $L_{Y,V}$, the normal wing-fuselage load $L_{Z,WF}$, the lateral wing-fuselage load $L_{Y,WF}$, and the rolling-moment contributions of the wing-fuselage and horizontal tail $(M_{X,WF} + M_{X,H})$.

$$\left. \begin{aligned} L_{Z,H} &= \frac{M_Y - (M_{Y,WF})_O - (L_{Z,A})(x_{Z,WF})}{x_H - x_{Z,WF}} \\ L_{Z,WF} &= \frac{(L_{Z,A})x_H - M_Y + (M_{Y,WF})_O}{x_H - x_{Z,WF}} = L_{Z,A} - L_{Z,H} \\ L_{Y,V} &= \frac{M_Z - (L_{Y,A})(x_{Y,WF})}{x_V - x_{Y,WF}} \\ L_{Y,WF} &= \frac{(L_{Y,A})x_V - M_Z}{x_V - x_{Y,WF}} = L_{Y,A} - L_{Y,V} \\ M_{X,WF} + M_{X,H} &= M_X + \frac{M_Z - (L_{Y,A})(x_{Y,WF})}{x_V - x_{Y,WF}} z_V \end{aligned} \right\} \quad (9)$$

By substituting equations (2) and (7) into equations (9) the following expressions for the component loads are obtained.

$$\begin{aligned}
 L_{Z,H} &= \frac{I_Y}{x_{t,H}} \dot{q} - \frac{(I_Z - I_X)}{x_{t,H}} pr - \frac{I_{XZ}}{x_{t,H}} (r^2 - p^2) + \frac{I_{X,e}}{x_{t,H}} \omega_{er} - \\
 &\quad \frac{(C_{m,WF})_0 S \bar{c}}{x_{t,H}} q_d - \frac{W \bar{c}}{g(x_{t,H})} \left[\frac{C_{m,WF} - (C_{m,WF})_0}{C_{N,WF}} \right] a_{Z,cg} \\
 L_{Z,WF} &= \frac{W x_H}{g(x_{t,H})} a_{Z,cg} - \frac{I_Y}{x_{t,H}} \dot{q} + \frac{(I_Z - I_X)}{x_{t,H}} pr + \frac{I_{XZ}}{x_{t,H}} (r^2 - p^2) - \\
 &\quad \frac{I_{X,e}}{x_{t,H}} \omega_{er} + \frac{(C_{m,WF})_0 S \bar{c}}{x_{t,H}} q_d \\
 L_{Y,V} &= \frac{I_Z}{x_{t,V}} \dot{r} - \frac{(I_X - I_Y)}{x_{t,V}} pq - \frac{I_{XZ}}{x_{t,V}} (\dot{p} - qr) - \frac{I_{X,e}}{x_{t,V}} \omega_{eq} - \\
 &\quad \frac{W b}{g(x_{t,V})} \left(\frac{C_{n,WF}}{C_{Y,WF}} \right) a_{Y,cg} \\
 L_{Y,WF} &= \frac{W x_V}{g(x_{t,V})} a_{Y,cg} - \frac{I_Z}{x_{t,V}} \dot{r} + \frac{(I_X - I_Y)}{x_{t,V}} pq + \frac{I_{XZ}}{x_{t,V}} (\dot{p} - qr) + \\
 &\quad \frac{I_{X,e}}{x_{t,V}} \omega_{eq} \\
 M_{X,WF} + M_{X,H} &= I_X \dot{p} - (I_Y - I_Z) qr - I_{XZ} (\dot{r} + pq) + (L_{Y,V}) z_V
 \end{aligned} \tag{9a}$$

The geometric, aerodynamic, and mass parameters which relate the airplane motions to the various loads are thus expressed in equations (9a).

The geometric parameters in equation (9a) are $x_{t,H}$, the distance between the aerodynamic center of the wing-fuselage combination (in pitch plane) and the aerodynamic center of the horizontal tail; $x_{t,V}$, the distance

between the aerodynamic center of the wing-fuselage combination (in yaw plane) and the aerodynamic center of the vertical tail; S , the wing area; \bar{c} , the mean aerodynamic chord; b , the wing span; x_H , the distance between the axis through the center of gravity and the chordwise aerodynamic center of the horizontal tail; x_V , the distance between the axis through the center of gravity and the chordwise aerodynamic center of the vertical tail; and z_V , the distance between the X body axis and the spanwise aerodynamic center of the vertical tail.

The aerodynamic characteristics required in equations (9a) are $C_{m,WF}$, the pitching-moment coefficient of the wing fuselage for the flight condition; $(C_{m,WF})_0$, the pitching-moment coefficient of the wing fuselage at zero normal force; $C_{N,WF}$, the normal-force coefficient of the wing-fuselage for the flight condition; $C_{n,WF}$, the yawing-moment coefficient of the wing fuselage for the flight condition; and $C_{Y,WF}$, the side-force coefficient of the wing fuselage for the flight condition.

The mass parameters required are the moments and products of inertia and the weight. The moments of inertia of the rotating parts of the engine $I_{X,e}$ and its rate of rotation ω_e are also required, if they are deemed to be significant.

For airplanes for which the pitching- and yawing-moment curves are known to be linear, the following substitutions may be made:

$$\left[\frac{C_{m,WF} - (C_{m,WF})_0}{C_{N,WF}} \right] = \left(\frac{\partial C_m}{\partial C_N} \right)_{WF} \quad (10)$$

$$\left(\frac{C_{n,WF}}{C_{Y,WF}} \right) = \left(\frac{\partial C_n}{\partial C_Y} \right)_{WF} \quad (11)$$

ACCURACY OF DETERMINING LOADS FROM BASIC MEASUREMENTS

As has been noted the geometric, aerodynamic, and mass parameters that occur in equations (9a) are required or may be used to determine

individual surface loads from the measured and directly derived quantities. The accuracy with which these surface loads may be determined depends on the accuracy with which the various parameters are known as well as on the accuracy of the measured and derived quantities. The effects of possible inaccuracies in the estimations of the various geometric, aerodynamic, and mass parameters used to obtain the loads have been determined by a series of calculations. (Instrument and recording errors have not been included in these calculations.) As an illustration, the accuracies with which the various parameters may be estimated are listed in table I for a fighter and for a bomber of contemporary design. The weights, moments of inertia, and center-of-gravity position are given for two conditions: one for which only a general knowledge of the mass and its distribution are known, that is, some average condition of the various possible flight conditions is used; and one for which the take-off weight, mass distribution, and their approximate variations with flight time are known for the specific flight being studied. These will be designated herein respectively as "unknown" and "known" loading conditions. The tail length also has two values corresponding to the known and unknown center-of-gravity positions. The errors in the aerodynamic parameters $(C_{m,WF})_0$, $x_{Z,WF}$, and $x_{Y,WF}$ were estimated from various existing comparisons between flight and wind-tunnel results and are representative of average errors which exist in these comparisons over the lift and Mach number range.

Two general flight conditions were assumed for the calculations - one, a violent maneuver for which large angular accelerations and velocities were used and which were considered to occur at the same time and in a direction to make the error maximum and the other, a gradual maneuver for which the angular motions were assumed to be zero. The flight conditions and airplane motions (Mach number, dynamic pressure, angular velocities and accelerations, and the ranges of normal and transverse accelerations) considered for the calculations are given in table II.

Not all the results of these calculations will be presented herein inasmuch as the general implications can be demonstrated by a few selected results and summary figures.

In figure 3 are shown the errors in the total normal force $L_{Z,A}$ for a fighter airplane, the normal force being directly derived from the measured quantities and the weight. The errors are caused by the inaccuracies in estimating the center-of-gravity position and the weight. Shown are the results for the unknown and known loading conditions and the very significant improvement resulting from the known condition. In figure 3 are variations with normal load factor n_Z of the percentage error of the total airplane normal force or load $L_{Z,A}$ and the error in this load as a proportion of the airplane weight. The maximum error

as a proportion of the weight varies from 0.2 at $n_z = 0$ to 1.0 at $n_z = 8$, whereas the corresponding percentage error varies from ∞ to 12 percent. It would appear that the error in proportion to the weight is more meaningful.

These errors are maximum, or almost ultimate, and occur only for the special conditions of the calculations, wherein maximum angular motions were assumed to occur and in such a direction as to cause the largest possible errors. Since the program is statistical, a more appropriate error would be an average or most probable error. Therefore, in figure 3 also shown are the approximate root-mean-square errors σ , which are the type of average errors normally considered in statistical studies. (For this paper it was assumed that the root-mean-square errors were one-third of the maximum errors.) For example, about 999 out of 1,000 errors might be less than the maximum and about 70 percent of all errors would be less than the root-mean-square error.

As noted before, there is a very obvious improvement in all errors when the loading condition is known. In this case, the known errors are smaller than the unknown errors by a factor of about 5.

The other directly derived loads, $L_{Y,A}$ for the fighter and $L_{Z,A}$ and $L_{Y,A}$ for the bomber, had errors of a similar order of magnitude to those shown in figure 3. For the total side loads $L_{Y,A}$, the error in pounds was about the same as that for the normal loads; however, the percentage errors were naturally larger than those for the normal loads since side-load factors are almost always less than one.

The horizontal-tail load can not be derived directly from the measured quantities, as is the total normal load, but depends on a knowledge of the geometric and aerodynamic parameters that occur in equations (9a). Calculations of the errors in the horizontal-tail load for the fighter airplane at subsonic speed are presented in figure 4. As in figure 3, the errors are shown as a percentage of the total load and as a proportion of the airplane weight. Because the root-mean-square errors are deemed to be most significant to the subject study, only those errors are shown. In general, the maximum errors for such indirectly derived loads as the horizontal-tail loads will be about three times as large as the root-mean-square errors. Results of both violent and gradual maneuvers for the unknown and known loadings are given in figure 4. It is of interest to note that, although the percentage errors for the two types of maneuvers are grossly different, the actual error in pounds is nearly the same. The very large percentage errors for the gradual maneuvers occur because the tail load itself is relatively small; this result, of course, reemphasizes the more significant value of the load error in pounds or in proportion to the airplane weight than in percentage of the

total load. For the two types of maneuvers with the unknown loading, the error in the horizontal-tail load ranged from about 0.005 to about 0.12 times the airplane weight. Errors about one-half as large were calculated for known than for unknown loading conditions. Thus, in evaluating a load not directly derivable from the measured quantities, such as the horizontal-tail load, a knowledge of the take-off loading improves the results significantly, although not to such a great extent as for directly derived loads such as the total normal load.

It should be pointed out that the percentage errors in horizontal-tail load for the gradual maneuvers are not always larger than those for violent maneuvers, as is the case for the preceding example at subsonic speeds. For the supersonic speed case studied, the percentage errors for the violent maneuvers are larger than those for the gradual maneuvers. This result occurs primarily because of the rearward shift of the aerodynamic center at the supersonic speeds. In general, however, the percentage errors of the tail loads at supersonic speeds were lower than at subsonic speeds for the conditions calculated.

Summaries of the root-mean-square errors of the horizontal- and vertical-tail loads in units of weight are presented in figures 5 and 6. On these figures are shown the effects of airplane type (fighter or bomber), type of maneuver (violent or gradual), and Mach number for known and unknown loading conditions. For the horizontal-tail load (fig. 5) the errors are generally larger at supersonic speeds than for subsonic speeds because of a rearward shift of the aerodynamic center of the normal load of the wing-fuselage combination. Little effect of Mach number was calculated for the vertical-tail load, and none is shown in figure 6 because the aerodynamic center of the lateral load of the wing-fuselage combination is little affected by Mach number. The errors in the horizontal-tail load in units of airplane weight are larger for the fighter than for the bomber because of the more violent maneuvering capabilities and the relatively smaller geometric characteristics of the fighter. These conclusions are, of course, based only on the calculations made herein; the results may be different for other flight conditions.

If the vertical-tail load errors in weight units (fig. 6) are considered, the fighter again has larger errors than does the bomber. The reasons are similar to those regarding the horizontal-tail load, but other flight conditions may bring about different results. For both the horizontal tail and vertical tail, the calculated maximum loads of the fighter were always larger in proportion to its weight than were those for the bomber. The percentage errors in tail load for the fighter, however, were not necessarily larger than those of the bomber.

As the error calculations are so closely related to the various characteristics of the airplane in question, the values shown herein

and the comments made are not specifically applicable to other airplanes. Each case requires its own careful error estimation.

The error calculations discussed have been for a direct application of the measured quantities and equations (9a) to obtain specific loads. For estimations of the probability distributions of the loads from the probability distributions of the measured quantities (noted in fig. 1), the same dimensional, mass, and aerodynamic characteristics as were used herein are required. It is believed, however, that the errors involved would be reflected to a lesser extent in the application of the probability distributions of the measured quantities to obtain probability distributions of loads. It is evident that such errors would affect the reliability or the confidence with which the probability distributions of the measured quantities are obtained. Thus, the reliability or confidence of the probability values of estimated loads would probably be reduced over that of the measured quantities. No estimations have been made of the effect of these errors on the probability distributions.

DERIVED PROBABILITY CURVES

In blocks numbered 14 to 16 of figure 1, it is indicated that the statistical probability curves for the basic parameters would be combined to obtain probability curves for the component loads. For example, the horizontal-tail load can be expressed in terms of the measured quantities from equation (9a) as

$$L_{Z,H} = C_1 q_d + C_2 n_Z + C_3 \dot{q} + C_4 p r + C_5 (r^2 - p^2) + C_6 \omega_e r \quad (12)$$

where the constants C_1, C_2, \dots are coefficients defined in equation (9a). The horizontal-tail load may be considered to be in two parts, the balancing- or level-flight tail load and the maneuvering tail load,

$$L_{Z,H} = (L_{Z,H})_{bal} + (L_{Z,H})_{man} \quad (13)$$

The balancing tail load is

$$(L_{Z,H})_{bal} = C_1 q_d + C_2 \quad (14)$$

The maneuvering tail load is

$$(L_Z, H)_{\text{man}} = C_2(n_Z - 1) + C_3\dot{q} + C_4pr + C_5(r^2 - p^2) + C_6\omega_e r \quad (15)$$

For each of the basic quantities in equation (12), there would be an associated probability curve. There is a possibility of combining these separate probability curves in order to obtain the resultant probability curve for the tail load. One of the important questions involved in combining probability curves is the possibility of a phase relationship or a correlation between the various parameters. For example, in a given maneuver there is certainly some degree of correlation or phase relationship between load factor n_Z and pitching acceleration \dot{q} . If a large number of maneuvers are considered, however, it is possible that the degree of correlation will become smaller or the phase relationships will become less important. If this were true, the calculation of the probability curves for tail load from those of the basic parameters would be greatly simplified.

In order to gain some insight into the calculation of probability curves of tail load from the basic parameters and to check into the degree of correlation between the parameters, probability curves were obtained for one operational training flight of a swept-wing fighter airplane. The flight chosen was a transition flight of about 1-hour duration which consisted of acrobatics, dive bombing, and ground strafing runs. Since the tail loads were not measured directly, a time history of the tail load was calculated for the complete flight by using equation (9a) except that, for simplicity, effects of rolling and yawing velocities were neglected ($p = r = 0$). In figure 7 are shown the probability curves for normal load factor, pitching acceleration, and dynamic pressure for the case chosen. Similarly, there would be probability curves for the other parameters making up the tail load; however, in this case, zero probability is assumed for these parameters since their effects were omitted in calculating the tail-load time history.

Since the horizontal-tail load is a function of the parameters shown in figure 7, the probability of exceeding a given tail load should be a function of these individual parameter probability curves

$$P(L_Z, H) = f[P(n_Z), P(\dot{q}), P(q_d)] \quad (16)$$

If the basic quantities were normally distributed and stochastically independent, the combination of the individual probability curves would be simplified. (See ref. 8.) For example, the distribution or probability

density function for a normally distributed variable with a mean \bar{y} and a standard deviation σ_y is

$$f\{y\} = \frac{1}{\sigma_y \sqrt{2\pi}} e^{-\frac{1}{2} \left(\frac{y-\bar{y}}{\sigma_y} \right)^2} \quad (17)$$

The probability density function for the tail load

$$L_{Z,H} = C_1 q_d + C_2 n_Z + C_3 \dot{q} \quad (18)$$

would then be normally distributed with a mean

$$\bar{L}_{Z,H} = C_1 \bar{q}_d + C_2 \bar{n}_Z + C_3 \bar{\dot{q}} \quad (19)$$

and a standard deviation

$$\sigma_{L_{Z,H}} = \left(C_1^2 \sigma_{q_d}^2 + C_2^2 \sigma_{n_Z}^2 + C_3^2 \sigma_{\dot{q}}^2 \right)^{1/2} \quad (20)$$

For normally distributed variables the theories may also be extended to stochastically dependent variables. (See ref. 8, for example.)

It can be observed from figure 7 that the probability curves of load factor and pitching acceleration are obviously not normally distributed. Therefore, equations (19) and (20) are not valid for the example problem.

In order to illustrate the method used in determining the probability curve of tail load from the probability curves of the individual parameters, the calculations for the maneuvering tail load will be described. If $p = r = 0$, the maneuvering tail load is

$$(L_{Z,H})_{\text{man}} = C_2 \Delta n_Z + C_3 \dot{q} = (L_{Z,H})_{\Delta n} + (L_{Z,H})_{\dot{q}} \quad (21)$$

If $f\{\Delta n\}$ and $f\{\dot{q}\}$ are the probability density functions of Δn and \dot{q} , the probability density functions of $(L_{Z,H})_{\Delta n}$ and $(L_{Z,H})_{\dot{q}}$ are

$$f\{(L_{Z,H})_{\Delta n}\} = \frac{f\{\Delta n\}}{C_2} \quad (22)$$

$$f\{(L_{Z,H})_{\dot{q}}\} = \frac{f\{\dot{q}\}}{C_3} \quad (23)$$

From this point it is advantageous to work with the functions of the incremental tail load due to Δn and due to \dot{q} given in equations (22) and (23).

As a first step, normal load factor and pitching acceleration were assumed to be independent. This assumption implies, for example, that for any constant value of the load factor the probability curve for pitching acceleration does not change. With the assumption of independence the joint density function of $(L_{Z,H})_{\Delta n}$ and $(L_{Z,H})_{\dot{q}}$ is

$$f\{(L_{Z,H})_{\Delta n}, (L_{Z,H})_{\dot{q}}\} = f\{(L_{Z,H})_{\Delta n}\} f\{(L_{Z,H})_{\dot{q}}\} \quad (24)$$

and

$$f\{(L_{Z,H})_{\Delta n}\} d(L_{Z,H})_{\Delta n} = P[(L_{Z,H})_{\Delta n}] \quad (25)$$

is the probability that a value of $(L_{Z,H})_{\Delta n}$ will occur in the interval $(L_{Z,H})_{\Delta n}$ and $(L_{Z,H})_{\Delta n} + d(L_{Z,H})_{\Delta n}$ and so forth. The probability of exceeding a given maneuvering tail load is then

$$P[(L_{Z,H})_{man}] = \int_{-\infty}^{\infty} \int_{(L_{Z,H})_{\Delta n}}^{\infty} f\{(L_{Z,H})_{\Delta n}, (L_{Z,H})_{\dot{q}}\} d(L_{Z,H})_{\Delta n} d(L_{Z,H})_{\dot{q}} \quad (26)$$

The distribution to be integrated is illustrated graphically in figure 8. The joint probability density function (eq. (24)) is plotted on the vertical scale with the incremental tail load due to load factor $(L_{Z,H})_{\Delta n}$ and the incremental tail load due to pitching acceleration $(L_{Z,H})_{\dot{q}}$ plotted on the other axes. Lines of constant tail load $(L_{Z,H})_{\text{man}}$ are represented by 45° lines (eq. (21)) as indicated in figure 8. The probability of exceeding a given maneuvering tail load is represented by the volume of the distribution falling outside the vertical plane represented by equation (21).

Inasmuch as the probability curves such as shown in figure 7 in many cases can not be expressed analytically, the calculations must be carried out numerically. The tail load $(L_{Z,H})_{\text{man}}$ and the tail-load increments $(L_{Z,H})_{\Delta n}$ and $(L_{Z,H})_{\dot{q}}$ are grouped into class intervals of equal size $\Delta L_{Z,H}$ and numbered consecutively $i, j = 0, 1, 2, 3, 4, \dots$ where

$$\left. \begin{aligned} (L_{Z,H})_{\text{man}} &= (i + j) \Delta L_{Z,H} \\ (L_{Z,H})_{\Delta n} &= i \Delta L_{Z,H} \\ (L_{Z,H})_{\dot{q}} &= j \Delta L_{Z,H} \end{aligned} \right\} \quad (27)$$

The probability that a value $(L_{Z,H})_{\Delta n, i}$ and $(L_{Z,H})_{\dot{q}, j}$ will occur together is

$$p \left\{ \left[(L_{Z,H})_{\Delta n} \right]_i, \left[(L_{Z,H})_{\dot{q}} \right]_j \right\} = p \left[(L_{Z,H})_{\Delta n} \right]_i p \left[(L_{Z,H})_{\dot{q}} \right]_j \quad (28)$$

The value of p obtained from the probability of exceeding curves P (fig. 7 and eqs. (22) or (23)) is

$$p(y)_i = P(y)_i - P(y)_{i+1} \quad (29)$$

The probability that a tail load $(L_{Z,H})_{\text{man}} = K \Delta L_{Z,H}$ will occur is then

$$P \left[(L_{Z,H})_{\text{man}} \right]_K = \sum_{i \text{ or } j=0}^{i+j=K} P \left\{ \left[(L_{Z,H})_{\Delta n} \right]_i, \left[(L_{Z,H})_{\dot{q}} \right]_j \right\}_{(i+j)=K} \quad (30)$$

The probability of exceeding a given maneuvering tail load is then obtained by summing equation (30) for all values of K

$$P \left[(L_{Z,H})_{\text{man}} \right]_K = \sum_{K=\infty}^K \sum_{i \text{ or } j=0}^{i+j=K} P \left\{ \left[(L_{Z,H})_{\Delta n} \right]_i, \left[(L_{Z,H})_{\dot{q}} \right]_j \right\}_{(i+j)=K} \quad (31)$$

$$P \left[(L_{Z,H})_{\text{man}} \right]_K = \sum_{K=\infty}^K \sum_{i \text{ or } j=0}^{i+j=K} \left\{ P \left[(L_{Z,H})_{\Delta n} \right]_i P \left[(L_{Z,H})_{\dot{q}} \right]_j \right\}_{(i+j)=K} \quad (31a)$$

By proceeding in a similar manner, the total horizontal-tail load probabilities were calculated and were based on the equation

$$f \left\{ (L_{Z,H})_{\Delta n}; (L_{Z,H})_{\dot{q}}; (L_{Z,H})_{q_d} \right\} = f \left\{ (L_{Z,H})_{\Delta n} \right\} f \left\{ (L_{Z,H})_{\dot{q}} \right\} f \left\{ (L_{Z,H})_{q_d} \right\} \quad (32)$$

The results of the calculations are shown in figure 9. In figure (9a) the maneuvering load above the 1 g balancing load is shown, and in figure (9b) the total tail load is shown. The symbols are the probabilities of exceeding a given tail load obtained by counting peaks from the time history of the calculated tail load. The lines are the probability curves derived from the probability curves of the individual parameters, independence being assumed. The agreement in both cases is excellent and confirms the assumption of independence for this one flight. In addition, correlation coefficients were computed between load factor and pitching acceleration for this flight and they also indicated a very low degree of correlation. Whether this will hold true in a more general case is not known. It is possible that there may be a high degree of correlation

in some cases, but at this time, it can only be said that for this one flight the simple methods work.

METHODS FOR DERIVING OPTIMUM DESIGN LOADS

In blocks numbered 16 to 18 in figure 1, it was indicated that the optimum design loads might be a function of the individual probability curves of all the component loads. In order to illustrate this condition, calculations were made for the optimum design horizontal and vertical tail loads for a hypothetical fighter airplane. (Some of the principles used in the method presented herein were first given in a paper presented at an IAS Specialist Meeting in Los Angeles, Calif. on August 23, 1955, by Innes Bouton and Dominic J. Scrooc of Northrup Aircraft Corporation entitled "A New Concept in Structural Design Criteria; Structural Reliability.")

The probability curve for the wing load factor used in these calculations (see ref. 4) is shown in figure 10. The tail-load probability curves are shown in figure 11. The horizontal-tail load curve was calculated for a typical fighter airplane from individual probability curves, as in figure 9. The vertical-tail load curve in figure 11 was arbitrarily assumed.

The probability of exceeding either the wing limit load, the horizontal-tail limit load, or the vertical-tail limit load may be expressed by the addition formula for probabilities (for example, see ref. 8):

$$P_{lim} = P\{WW_{lim}\} + P\{HH_{lim}\} + P\{VV_{lim}\} - P\{WW_{lim}HH_{lim}\} - P\{WW_{lim}VV_{lim}\} - P\{HH_{lim}VV_{lim}\} + P\{WW_{lim}HH_{lim}VV_{lim}\} \quad (33)$$

For example, the term $P\{WW_{lim}\}$ represents the probability that a peak wing load $L_{Z,W}$ will occur and that the wing load will be greater than the wing limit load; the term $P\{WW_{lim}HH_{lim}\}$ represents the probability that a peak wing load $L_{Z,W}$ and a peak horizontal-tail load $L_{Z,H}$ will occur at the same time and that both loads will exceed their respective limit loads, and so forth.

The probability of a given component load occurring and the probability that the load will exceed the limit load are independent so that $P\{WW_{lim}\} = P\{W\}P\{W_{lim}\}$. If it is assumed, in addition, that the

probability of exceeding the limit load of one component is independent of the probability of exceeding the limit load of another component then $P\{W_{lim}H_{lim}\} = P\{W_{lim}\}P\{H_{lim}\}$ and so forth and equation (33) becomes

$$\begin{aligned} P_{lim} = & P\{W\}P\{W_{lim}\} + P\{H\}P\{H_{lim}\} + P\{V\}P\{V_{lim}\} - P\{WH\}P\{W_{lim}\}P\{H_{lim}\} - \\ & P\{WV\}P\{W_{lim}\}P\{V_{lim}\} - P\{HV\}P\{H_{lim}\}P\{V_{lim}\} + \\ & P\{WHV\}P\{W_{lim}\}P\{H_{lim}\}P\{V_{lim}\} \end{aligned} \quad (33a)$$

The probabilities $P\{WHV\}$ and $P\{WH\}$ are probably dependent since the occurrence of a wing load is usually accompanied by the occurrence of a horizontal-tail load. The probabilities $P\{WV\}$ and $P\{HV\}$, however, are probably close to being independent and therefore may be expressed approximately as the products of the individual probabilities:

$$\left. \begin{aligned} P\{WV\} &\approx P\{W\}P\{V\} \\ P\{HV\} &\approx P\{H\}P\{V\} \end{aligned} \right\} \quad (34)$$

If it is further assumed that

$$P\{WHV\} \approx P\{WH\}P\{V\} \quad (35)$$

then it may be shown that

$$P\{WH\} \approx P\{W\} + P\{H\} - 1 \quad (35a)$$

The probability curves shown in figures 10 and 11 are based on the total number of load peaks exceeding some low threshold value of the wing or tail load, and the number of peak loads obtained in a given period of time will generally be different for the various components. If the average number of load experiences (wing, horizontal tail, vertical tail, or combinations of these component loads) is N/T per hour, the ratios of the average number of wing, horizontal-tail and vertical-tail loads per hour to the total number of loads per hour N/T are equal to the probabilities of the occurrence of the component loads and are

$$\left. \begin{aligned} f_W &= P\{W\} = \frac{N_W/T}{N/T} \\ f_H &= P\{H\} = \frac{N_H/T}{N/T} \\ f_V &= P\{V\} = \frac{N_V/T}{N/T} \end{aligned} \right\} \quad (36)$$

Equation (33a) with the assumptions of equations (34) and (35) may then be expressed as

$$P_{lim} = P\{W_{lim}\}f_W + P\{V_{lim}\}f_V \left(1 - P\{W_{lim}\}f_W\right) + \\ P\{H_{lim}\} \left\{ \left[f_H - P\{W_{lim}\}(f_W + f_H - 1) \right] \left(1 - P\{V_{lim}\}f_V\right) \right\} \quad (37)$$

or

$$P_{lim} = P\{W_{lim}\}f_W + P\{H_{lim}\} \left[f_H - P\{W_{lim}\}(f_W + f_H - 1) \right] + \\ P\{V_{lim}\}f_V \left[1 - P\{W_{lim}\}f_W - P\{H_{lim}\}f_H + P\{W_{lim}\}P\{H_{lim}\}(f_W + f_H - 1) \right] \quad (37a)$$

In the following example, it will be assumed that the optimum wing limit load factor has been selected as 7g by using methods such as those indicated in reference 1. These methods are based on the mission requirements and statistical data on existing airplanes. From figure 10 the probability of exceeding the limit wing load factor is

$$P\{W_{lim}\} = 0.0013$$

It is further assumed that the values of f are

$$f_W = 0.6$$

$$f_H = 0.9$$

$$f_V = 0.1$$

The values of f_W and f_H are based on results from a small sample of experimental data. The value of f_V is arbitrarily assumed.

Equations (37) and (37a) then become

$$P_{lim} = 0.00078 + 0.099922P\{V_{lim}\} + 0.89935\left(1 - 0.1P\{V_{lim}\}\right)P\{H_{lim}\} \quad (37b)$$

$$P_{lim} = 0.00078 + 0.89935P\{H_{lim}\} + 0.099922\left(1 - 0.900052P\{H_{lim}\}\right)P\{V_{lim}\} \quad (37c)$$

The probability of exceeding either the wing, horizontal-tail, or vertical-tail limit load is then calculated from equation (37b) at several constant values of the limit vertical-tail load with the limit horizontal-tail load as the variable. The values of the probabilities used in equation (37b) were obtained from figure 11. The results of this operation are shown in figure 12. From this figure it is evident that, for a given limit vertical-tail load, there is a value of the limit horizontal-tail load beyond which the probability does not decrease appreciably. If the optimum tail load is arbitrarily selected as the load where the probability is 5 percent greater than the minimum probability for infinite tail load, then

$$P_{lim}(L_{Z,H} = \infty) = P\{W_{lim}\}f_W + P\{V_{lim}\}f_V\left(1 - P\{W_{lim}\}f_W\right) \quad (38)$$

$$P_{lim}(L_Y, V = \infty) = P\{W_{lim}\}f_W + P\{H_{lim}\}\left[f_H - P\{W_{lim}\}(f_W + f_H - 1)\right] \quad (38a)$$

and

$$P_{lim,opt,H} = 1.05P_{lim}(L_Z, H = \infty) \quad (39)$$

$$P_{lim,opt,V} = 1.05P_{lim}(L_Y, V = \infty) \quad (39a)$$

In figure 12 the optimum limit horizontal-tail load for each selected limit vertical-tail load is indicated with a symbol. For example, the optimum limit horizontal-tail load is 7,850 pounds for an infinite limit vertical-tail load.

In a similar manner the optimum limit vertical-tail load may be determined at selected values of the limit horizontal-tail load by using equations (37c) and (39a).

In figure 13 the results of both calculations are shown. The variation of the optimum limit horizontal-tail load with limit vertical-tail load was obtained from figures 11 and 12. The other line is the variation of the optimum limit vertical-tail load with limit horizontal-tail load. The intersection of these two curves represents the optimum value of the limit horizontal- and limit vertical-tail loads. In this hypothetical case the optimum horizontal-tail limit load is 7,750 pounds and the optimum vertical-tail limit load is 2,750 pounds.

Although the method indicated and the curves shown in figure 13 are illustrative of the derivation of optimum design loads, the optimum loads can be more easily derived through an iteration procedure by using equations (37), (38), and (39).

The value of the probability of exceeding the optimum limit horizontal-tail load is

$$P\{H_{lim}\}_{opt} = \frac{0.05\left[P\{W_{lim}\}f_W + P\{V_{lim}\}f_V\left(1 - P\{W_{lim}\}f_W\right)\right]}{f_H - P\{W_{lim}\}(f_W + f_H - 1) - P\{V_{lim}\}f_V\left[f_H - P\{W_{lim}\}(f_W + f_H - 1)\right]} \quad (40)$$

The probability of exceeding the optimum limit vertical-tail load is

$$P\{V_{lim}\}_{opt} = \frac{0.05 \left\{ P\{W_{lim}\} f_W + P\{H_{lim}\} \left[f_H - P\{W_{lim}\} (f_W + f_H - 1) \right] \right\}}{f_V \left[1 - P\{W_{lim}\} f_W - P\{H_{lim}\} f_H + P\{W_{lim}\} P\{H_{lim}\} (f_W + f_H - 1) \right]} \quad (40a)$$

As a first step the limit vertical-tail load can be assumed to be infinite ($P\{V_{lim}\} = 0$) in which case

$$P\{H_{lim}\}_{opt} = \frac{0.05 P\{W_{lim}\} f_W}{f_H - P\{W_{lim}\} (f_W + f_H - 1)} \quad (40b)$$

This value of $P\{H_{lim}\}_{opt}$ from equation (40b) is then substituted into equation (40a) and a new value of $P\{V_{lim}\}_{opt}$ is calculated. The new value of $P\{V_{lim}\}_{opt}$ is then substituted into equation (40) to determine another value of $P\{H_{lim}\}_{opt}$ and so forth until the calculations converge; this convergence will usually be quite rapid. For the example given, the results are as follows:

Assume

$$P\{V_{lim}\}_{opt,1} = 0$$

thus from equation (40b),

$$P\{H_{lim}\}_{opt,1} = 0.00004336$$

from equation (40a),

$$P\{V_{lim}\}_{opt,2} = 0.0004098$$

from equation (40),

$$P\{H_{lim}\}_{opt,2} = 0.00004564$$

from equation (40a),

$$P\{V_{lim}\}_{opt,3} = 0.0004109$$

and from equation (40),

$$P\{H_{lim}\}_{opt,3} = 0.00004565$$

Thus from figure 11 it may be seen that the optimum horizontal-tail limit load corresponding to these iterated probabilities is 7,750 pounds and the optimum vertical-tail limit load is 2,750 pounds; these values are the same as those found in figure 13. As a matter of interest, the limit horizontal-tail load selected on the basis of present design criteria would be about 15,000 pounds for the airplane used in the example problem. Because of the limited nature of this example, it is not intended to imply that the present design criteria are generally conservative, for in some cases the optimum limit loads as derived from this method could be higher than the design loads selected on the basis of present criteria. The example is given here only to show a possible method of using the statistical data in developing design criteria.

Another way to select the limit tail load would be to select equal probability values for wing and tail. The probability of exceeding the limit wing load was $P\{W_{lim}\} = 0.0013$. If the same probability is selected for the tail load, it can be seen in figure 11 that a limit horizontal-tail load of 4,400 pounds and a limit vertical-tail load of 2,600 pounds would be selected. When these values are compared with the optimum values, it would seem that the "equal probability" criterion might lead to unconservative design and that the design of each of the components should be based on the optimum limit load which is a function of the combined probability distributions of the component loads. It must be remembered,

however, that these conclusions are based on statistical independence which has not been proved or disproved at the present time.

SAMPLE SIZE

One of the important problems in a statistical program is the determination of the sample size needed to define adequately the probability curves. The problem of selecting a sample size is a complex one and can not be answered without making assumptions about the reliability required.

The end results of this statistical analysis are in the form of probability curves. The degree of accuracy demanded for these curves dictates the sample size that is needed. In order to specify the degree of accuracy, confidence bands may be used as shown in the example given in figure 14. In figure 14 a typical probability curve is shown with 95-percent confidence bands. Confidence bands are shown for a sample size of 40 data peaks, 250 data peaks, 4,000 data peaks, and 64,000 data peaks. These confidence bands may be interpreted crudely in this manner: If many samples of the same size (that is, 40, 250, 4,000, or 64,000) were taken in similar operations, 95 percent of the time the probability curve obtained would fall within the confidence bands.

One of the things that could be specified in order to determine the sample size would be the spread in probability of the confidence bands at a given probability level. For example, in figure 14 the spread (taken as the increment between the probability curve and the upper confidence limit) indicated for the sample size of 4,000 points is about 100 percent at a probability level of 0.002. This 100-percent spread in the probability however means a maximum spread of only about 10 percent in load for this particular confidence band.

The 95 percent confidence limits can be given as in reference 8:

$$\frac{P'}{P' + (1 - P' + 1/N)v_{P_2}^2} < P < \frac{(P' + 1/N)v_{1-P_1}^2}{1 - P' + (P' + 1/N)v_{1-P_1}^2} \quad (41)$$

where $v_{P_2}^2$ and $v_{1-P_1}^2$ are variance ratios. (For example, see table VII in ref. 8)

$$v_{P_2}^2 = f(f_{1,P_2}, f_{2,P_2}) \quad (42)$$

$$v_{1-P_1}^2 = f(f_{1,1-P_1}, f_{2,1-P_1}) \quad (43)$$

where

$$f_{1,P_2} = 2N(1 - P' + 1/N) \quad (44)$$

$$f_{2,P_2} = 2NP' \quad (45)$$

$$f_{1,1-P_1} = 2N(P' + 1/N) \quad (46)$$

$$f_{2,1-P_1} = 2N(1 - P') \quad (47)$$

The percent spread in the confidence interval on the upper side (between the probability curve and the upper confidence band) is then

$$100 \frac{\Delta P'}{P'} = \frac{100(1 + 1/NP')v_{1-P_1}^2}{1 - P' + (P' + 1/N)v_{1-P_1}^2} - 1 \quad (48)$$

The percent spread in the probability values for the confidence interval on the upper side is shown plotted against the total number of data peaks N in figure 15 for several probability levels. For example, in figure 15 it can be seen that, if a 10 percent spread in the confidence interval at a probability level of 1 in 100,000 is required, about 40,000,000 data peaks are needed, whereas for a 400 percent spread at a probability level of 1 in 100, only about 100 data peaks would be required.

It might be desirable to determine the sample size by specifying the spread in the confidence interval at the probability level for limit loads. For example, the probability at limit wing load factor for current

fighter airplanes is about 1 in 1,000. A plot is shown in figure 16 of the maximum percent spread in load factor at limit load against the maximum percent spread in the probability values for the 95-percent confidence interval at a probability level of 1 in 1,000. This spread in the load for a given spread in the probability is a function of the shape of the probability curve; therefore, an approximate range of this spread is included in figure 16. The curve shown was obtained from figure 14 and the range of spread shown was estimated from available probability curves for various airplane parameters. From experience in analyzing statistical data, it has been found that a spread of about 150 percent in the probability values at large loads is generally satisfactory. At this level, it may be seen in figure 16 that the spread in the load is between 12 and 50 percent (about 25 percent for the curve of fig. 14). Therefore, if a spread of 150 percent in probability at a probability level of 1 in 1,000 is taken as a tentative figure, it can be seen in figure 15 that about 4,000 data peaks would be needed to define the probability curve for one quantity.

The manner in which the data are sorted would affect the sample size. At this time, it appears that probability distributions of each quantity for 10 altitude and 10 airspeed or Mach number intervals may suffice to cover the flight regime. Thus, each quantity that is measured would be sorted into 10 altitude intervals and, in turn, the data in each altitude interval would be sorted into 10 airspeed or Mach number intervals. This condition indicates that 100 data peaks are needed to assure an average of 1 data peak in each interval. It was indicated in figure 15 that 4,000 data peaks are needed to define a probability curve for the selected accuracy. Therefore, the total number of data peak values needed to cover the flight regime is $100 \times 4,000$ or 400,000. It is obvious that the accuracy or statistical reliability will be much higher for the total probability curve (marginal distribution) for all Mach numbers and altitudes which would be obtained from this total number of data peaks.

It is difficult to say what these 400,000 data peaks might mean in terms of airplane flight time but some guesses may be made. For example, these data might be obtained in about 200,000 hours of flight for large bombers. This time might represent about four years of flying with 50 instrumented airplanes. For a fighter, 400,000 peaks may represent about 25,000 hours of flight time and might require about 2 years of flying with 50 instrumented airplanes.

These estimated sample sizes are large and the processing and analysis of this amount of data might prove to be prohibitive, in which case further compromises in the statistical reliability would be necessary. For example, if the desired reliability were required only in the central ranges of airspeeds and altitudes in which 50 percent of the data were concentrated the sample estimates could then be reduced to about 100,000 data peaks. (In making such a compromise the reliabilities at the

lowest and highest airspeed and altitude ranges would be considerably reduced.) In this case this amount of data might be collected in approximately 50,000 hours for bombers and about 6,200 hours for fighter type airplanes.

Needless to say, the problem of selecting a sample size is a complex one and the numbers given herein are not necessarily what may actually be required. Variations of the order of 3 to 1 or more are common in such estimations and should be borne in mind.

CONCLUDING REMARKS

A study of methods of analyzing data obtained in a statistical maneuver-loads program has been made. This study indicates that the loads on the wing and tail surfaces may be derived from the basic measurements of the impact and static pressures, the three linear accelerations, and the three angular accelerations. In addition, a method of combining individual probability curves for the basic measured parameters to obtain probability curves for component loads is given and agrees with a small sample of data for one airplane. Also, a method for deriving optimum design loads for use in design criteria is presented. A rough estimation of the sample size necessary for a statistical flight program is also given.

The methods used and the results possible from such a statistical program as presented in this paper represent a possible goal which could be obtained under the assumption made; however, there are many phases of the program which require further study. An actual statistical program could differ in many respects to that presented, such differences depending in part upon the type and accuracy of the recording equipment.

Langley Aeronautical Laboratory,
National Advisory Committee for Aeronautics,
Langley Field, Va., May 28, 1957.

REFERENCES

1. Mayer, John P., and Hamer, Harold A.: A Study of Means for Rationalizing Airplane Design Loads. NACA RM L55E13a, 1955.
2. Freudenthal, A. M.: Safety and the Probability of Structural Failure. Proc. American Soc. Civ. Eng., vol. 80, no. 468, Aug. 1954, pp. 468-1 - 468-46.
3. Bronn, Carl E.: Some Aspects of Prediction of Load Spectrum for Airplanes. Presented to Fifth Meeting of the Structures and Materials Panel of AGARD (Copenhagen, Denmark), Apr. 29 to May 4, 1957.
4. Mayer, John P., Hamer, Harold A., and Huss, Carl R.: A Study of the Use of Controls and the Resulting Airplane Response During Service Training Operations of Four Jet Fighter Airplanes. NACA RM L53L28, 1954.
5. Mayer, John P., and Hamer, Harold A.: Applications of Power Spectral Analysis Methods to Maneuver Loads Obtained on Jet Fighter Airplanes During Service Operations. NACA RM L56J15, 1957.
6. Gray, Frank P.: Maneuver Load Data From Jet-Fighter Combat Operations. WADC-TN-55-12, Wright Air Dev. Center, U. S. Air Force, May 1955.
7. Mayer, John P., and Hamer, Harold A.: The Frequency Content of the Control Input and Airplane Response Obtained During Service Operations of Fighter Airplanes. NACA RM L57E21, 1957.
8. Hald, A.: Statistical Theory With Engineering Applications. John Wiley & Sons, Inc., c. 1952.

TABLE I.- ESTIMATED ERRORS USED IN CALCULATIONS

Airplane parameters	Error given in -	Fighter		Bomber	
		Loading unknown	Loading known	Loading unknown	Loading known
Weight	Percent	10	2	10	2
Center of gravity	Percent chord	5	1	5	1
Tail length, (x_t , x_H , and x_V)	Percent	5	3	3	2
I_X , I_Y , I_Z , I_{XZ} , $I_{X,e}$	Percent	5	3	15	9
$(C_{m,WF})_0$	Percent	20	20	20	20
x_Z, WF	Percent chord	3	3	4	4
x_Y, WF	Percent wing span	20	20	20	20

TABLE II.- FLIGHT CONDITIONS AND VALUES OF
MOTIONS USED IN ERROR CALCULATIONS

Quantity	Fighter		Bomber	
M	0.8, 2.0		0.8, 1.5	
q _d	500, 1,500		300, 700	
n _Z	-1 to 8		0 to 4	
n _Y	0 to 1.0		0 to 0.2	
	Value for -		Value for -	
	Violent	Gradual	Violent	Gradual
p	5	0	0.5	0
q	1.5	0	.2	0
r	0.75	0	.15	0
\dot{p}	10	0	.8	0
\dot{q}	6	0	.6	0
\dot{r}	3	0	.2	0

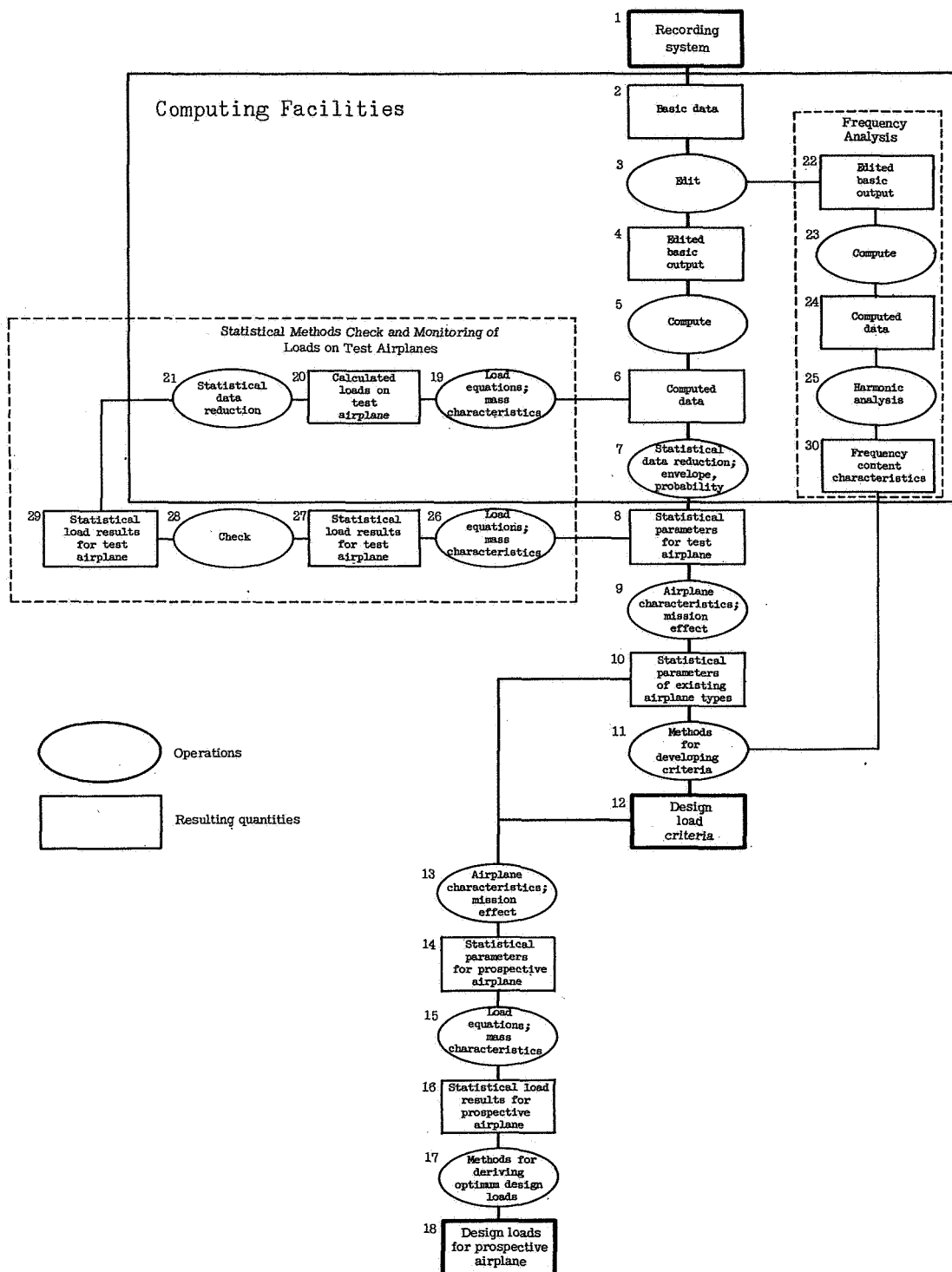


Figure 1.- Tentative outline for a large-scale statistical loads program.

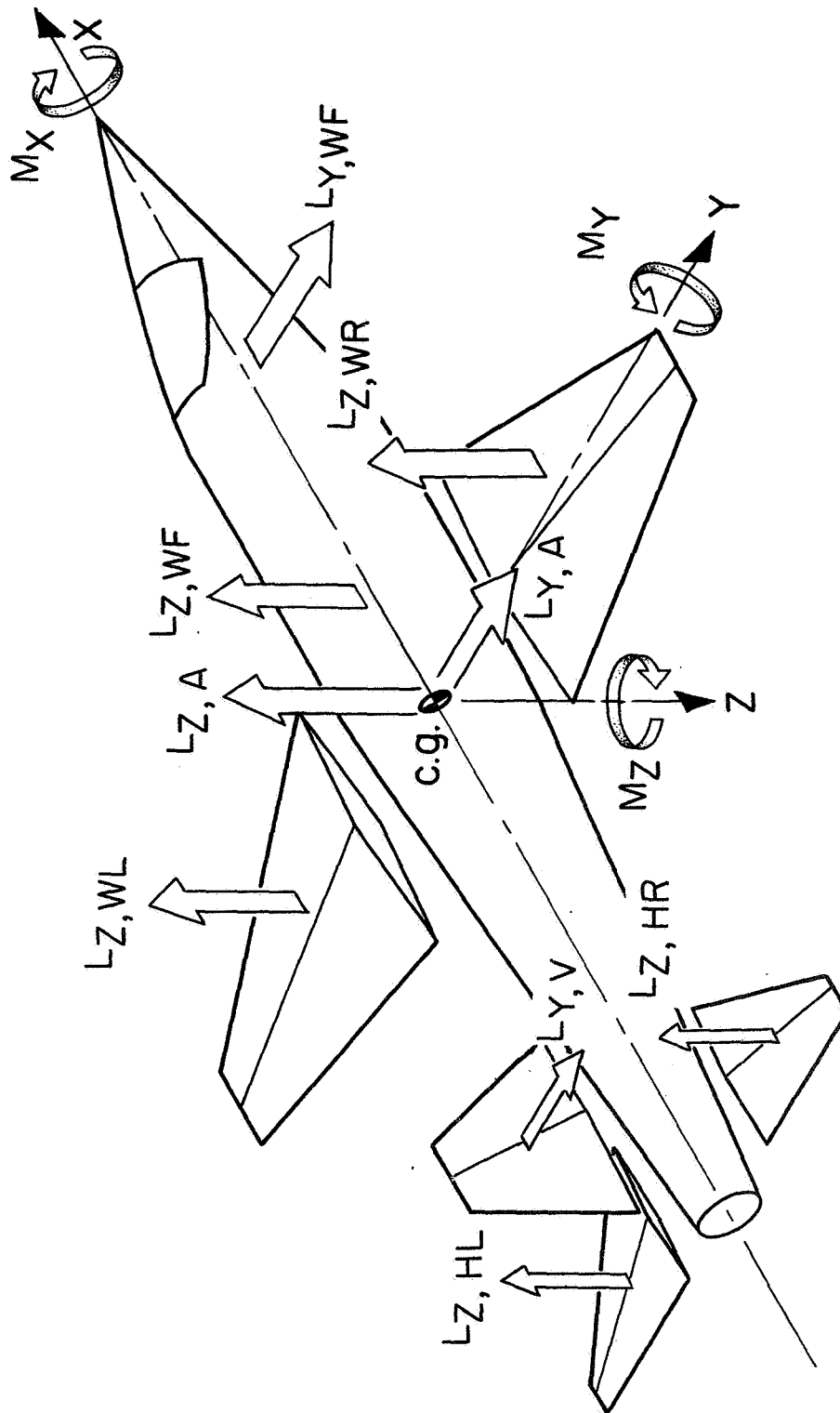
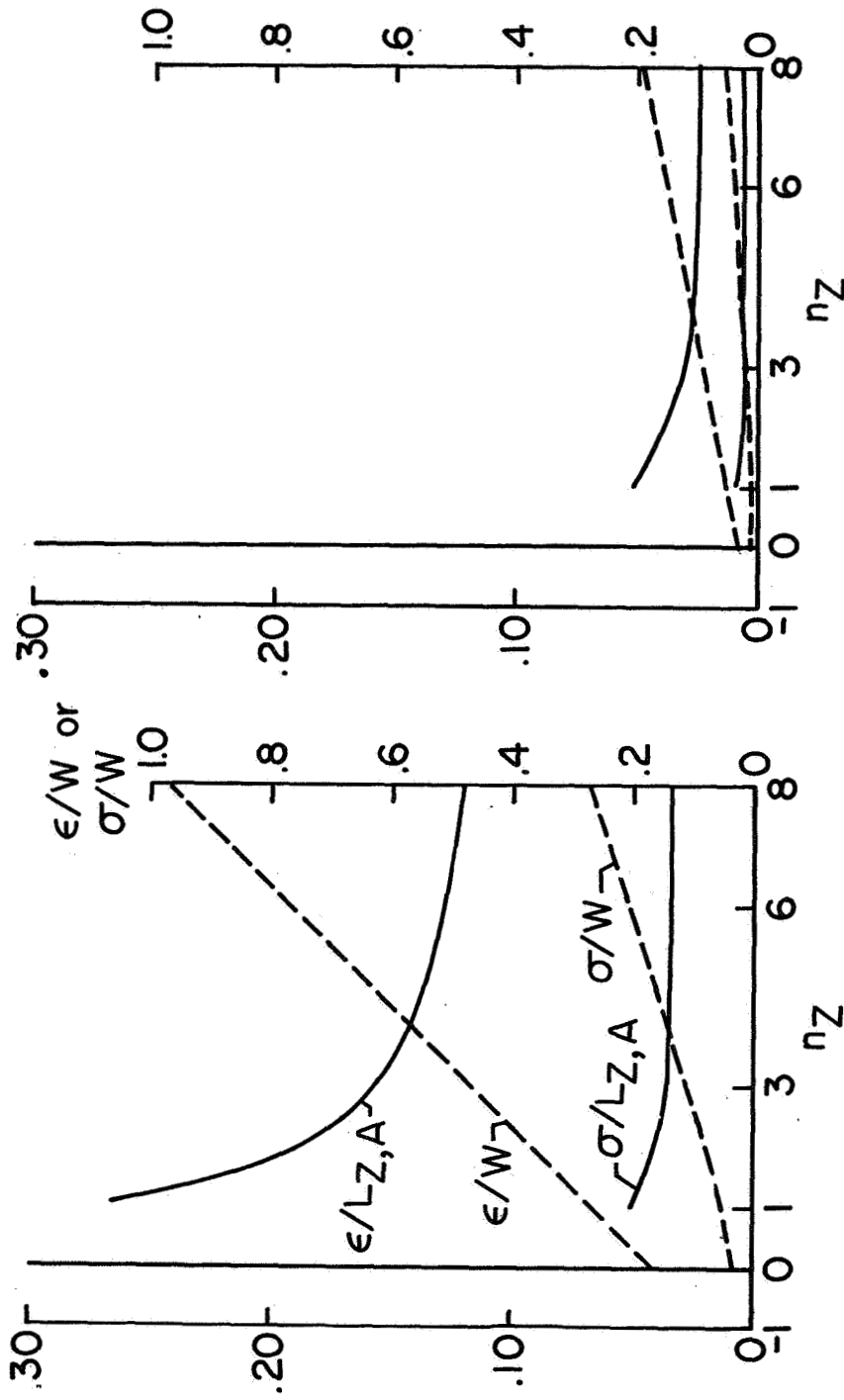


Figure 2.- Major load components on airplane. Arrows indicate positive distances from center of gravity, positive directions of loads, and positive moments.

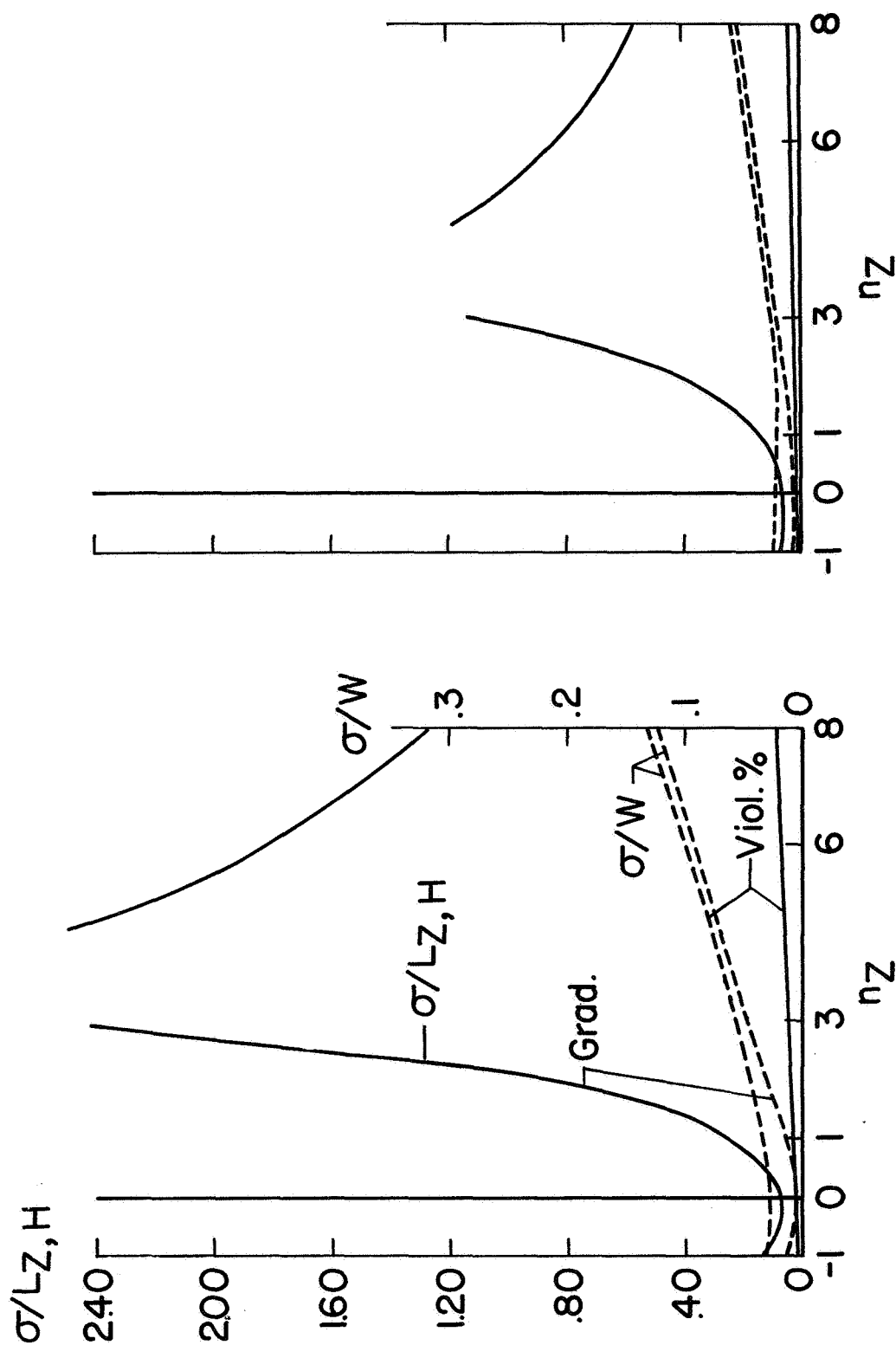
$\epsilon/L_{Z,A}$ or
 $\sigma/L_{Z,A}$



(a) Unknown take-off loading.

(b) Known take-off loading.

Figure 3.- Error in normal force due to inaccuracies in the knowledge of weight and location of the center of gravity. Fighter airplane.



(a) Unknown take-off loading.

(b) Known take-off loading.

Figure 4.- Error in horizontal-tail load at subsonic Mach numbers due to inaccuracies in the knowledge of mass and aerodynamic parameters. Fighter airplane.

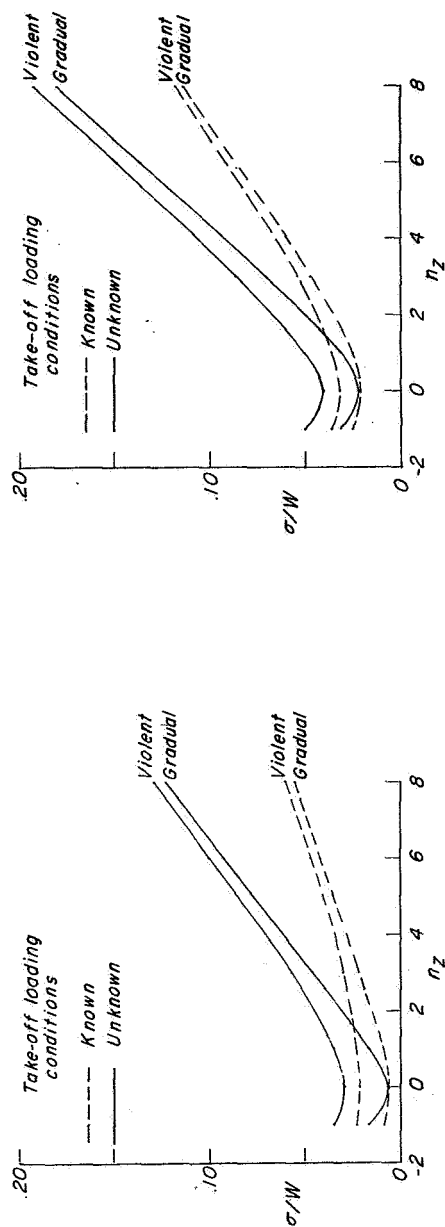
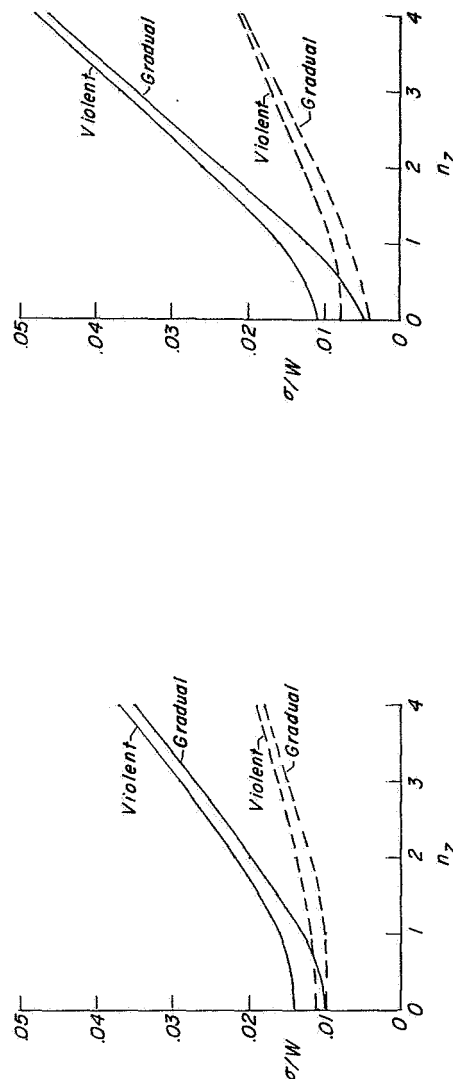
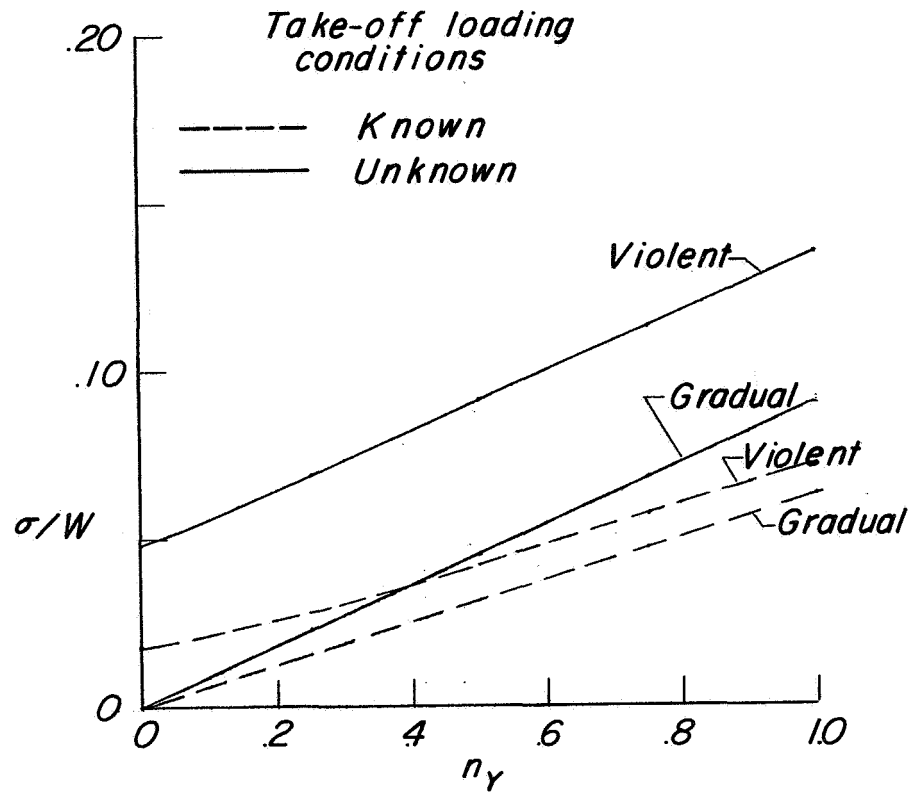
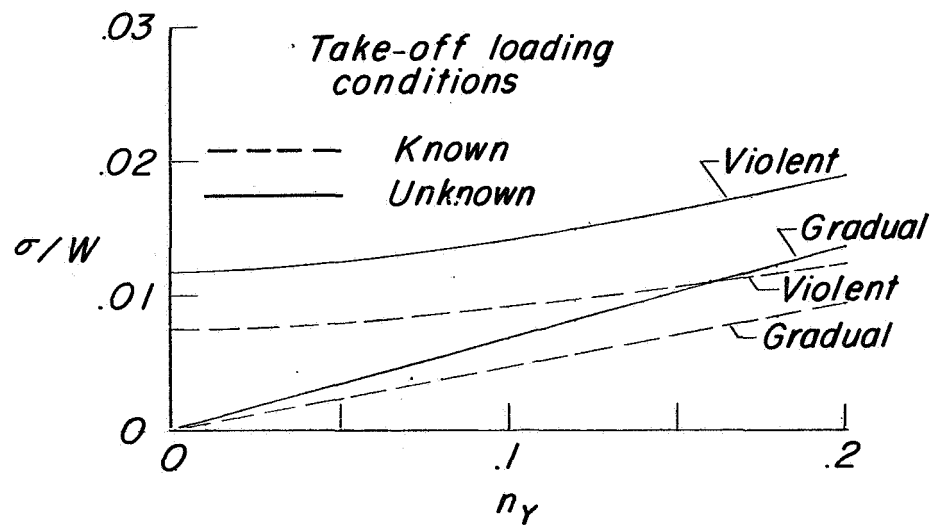
(a) Fighter airplane. $M < 1$.(b) Fighter airplane. $M > 1$.(c) Bomber airplane. $M < 1$.(d) Bomber airplane. $M > 1$.

Figure 5.- Influence of Mach number and airplane and maneuver type on the root-mean-square errors in horizontal-tail load.



(a) Fighter airplane.



(b) Bomber airplane.

Figure 6.- Influence of airplane and maneuver type on the root-mean-square errors in vertical-tail loads at subsonic Mach numbers.

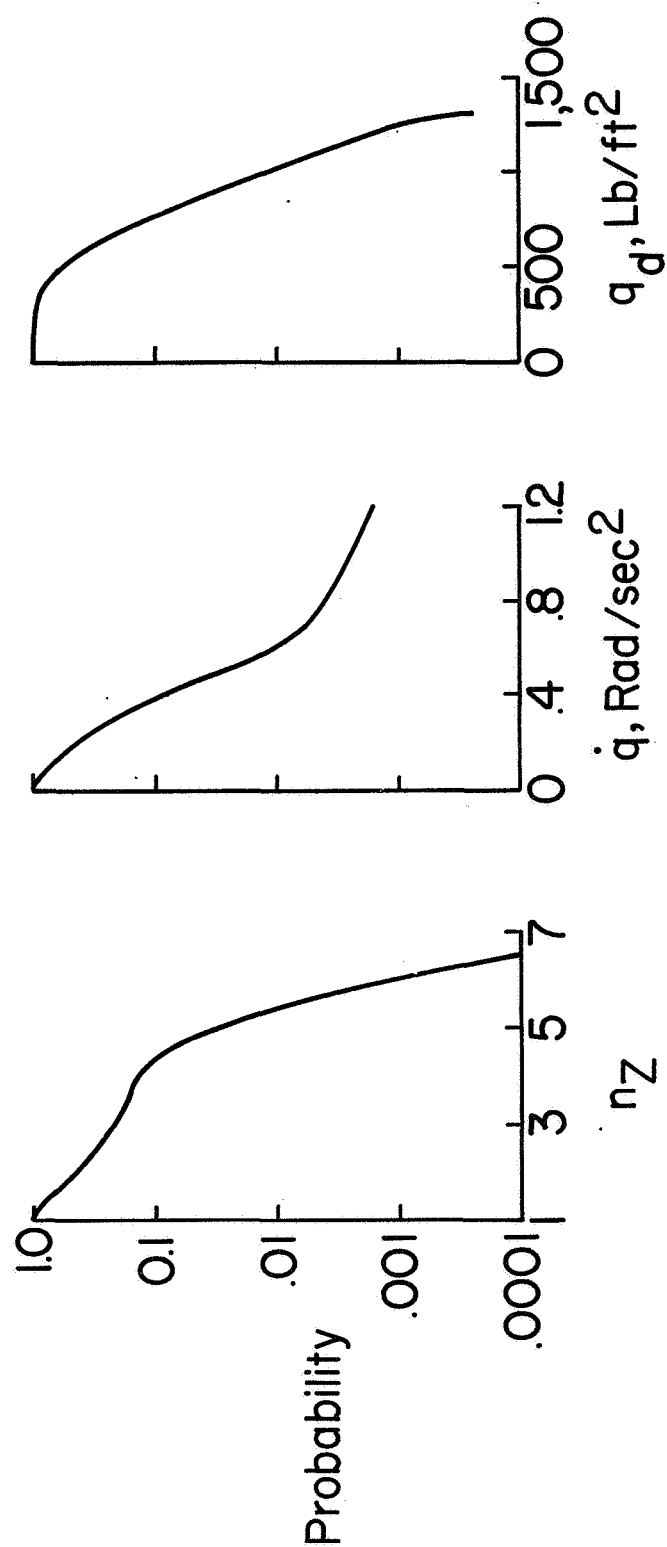


Figure 7.- Probability curves for normal load factor, pitching acceleration, and dynamic pressure for one operational flight of a swept-wing fighter airplane.

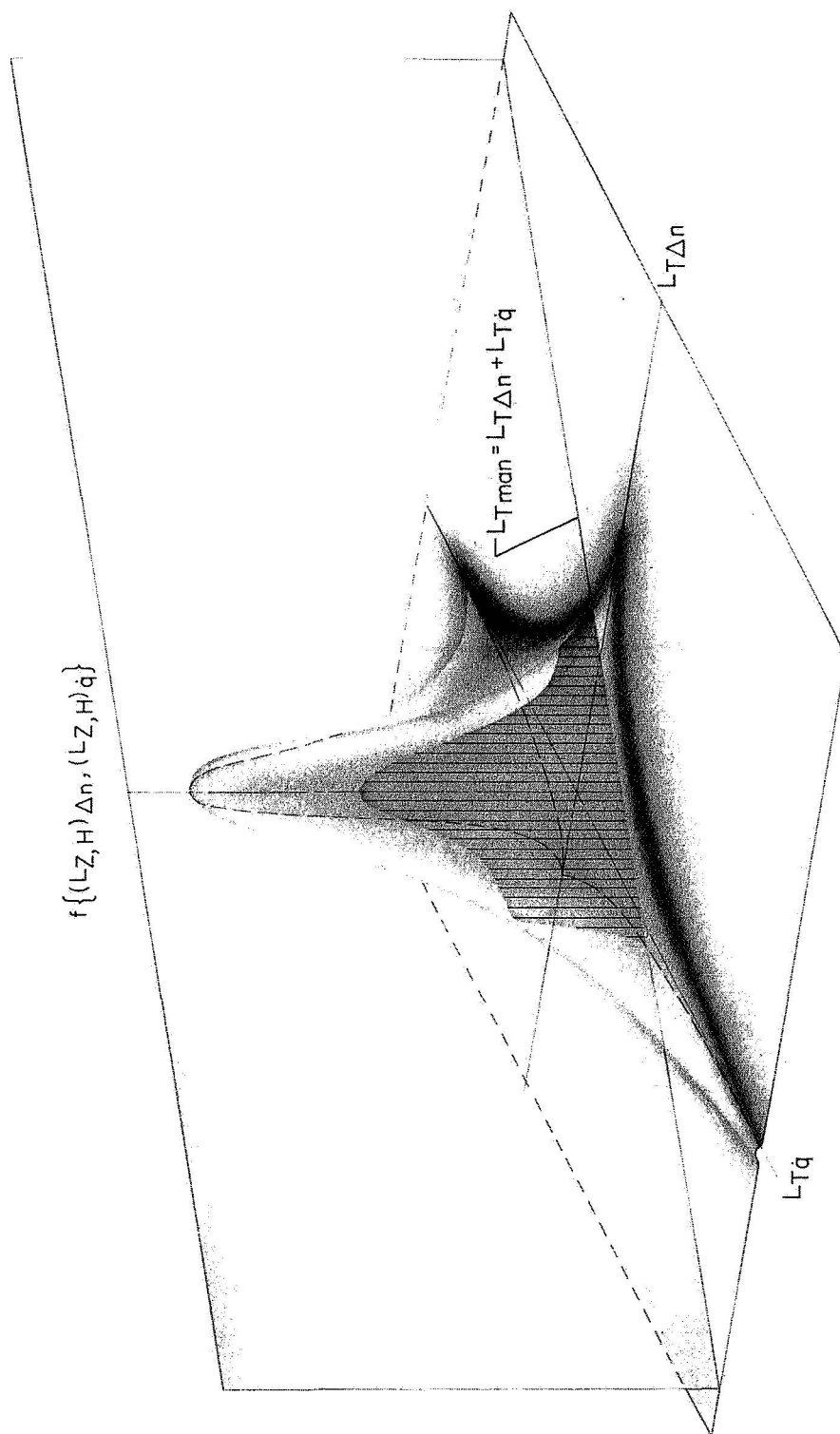


Figure 8.- Pictorial representation of joint density function $f\{(L_Z, H)_{\Delta n}, (L_Z, H)_{\dot{q}}\}$ used to obtain probability of exceeding a given maneuvering horizontal-tail load,

$$P[(L_Z, H)_{\text{man}}] = \int_{-\infty}^{\infty} \int_{-\infty}^{\infty} f\{(L_Z, H)_{\Delta n}, (L_Z, H)_{\dot{q}}\} d(L_Z, H)_{\Delta n} d(L_Z, H)_{\dot{q}}$$

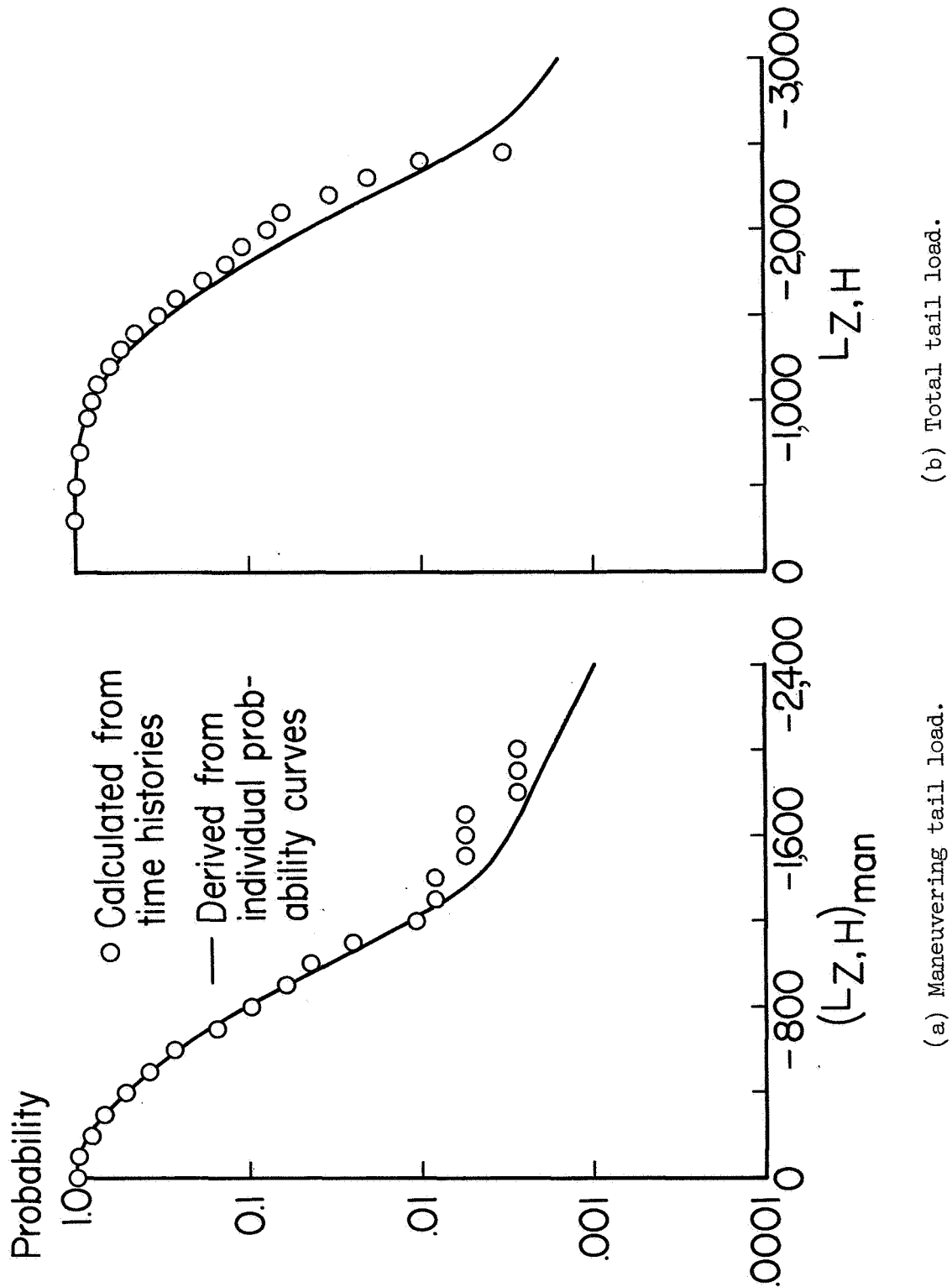


Figure 9.- Comparison of measured and derived probability curves for horizontal-tail load for one operational flight of a swept-wing fighter airplane.

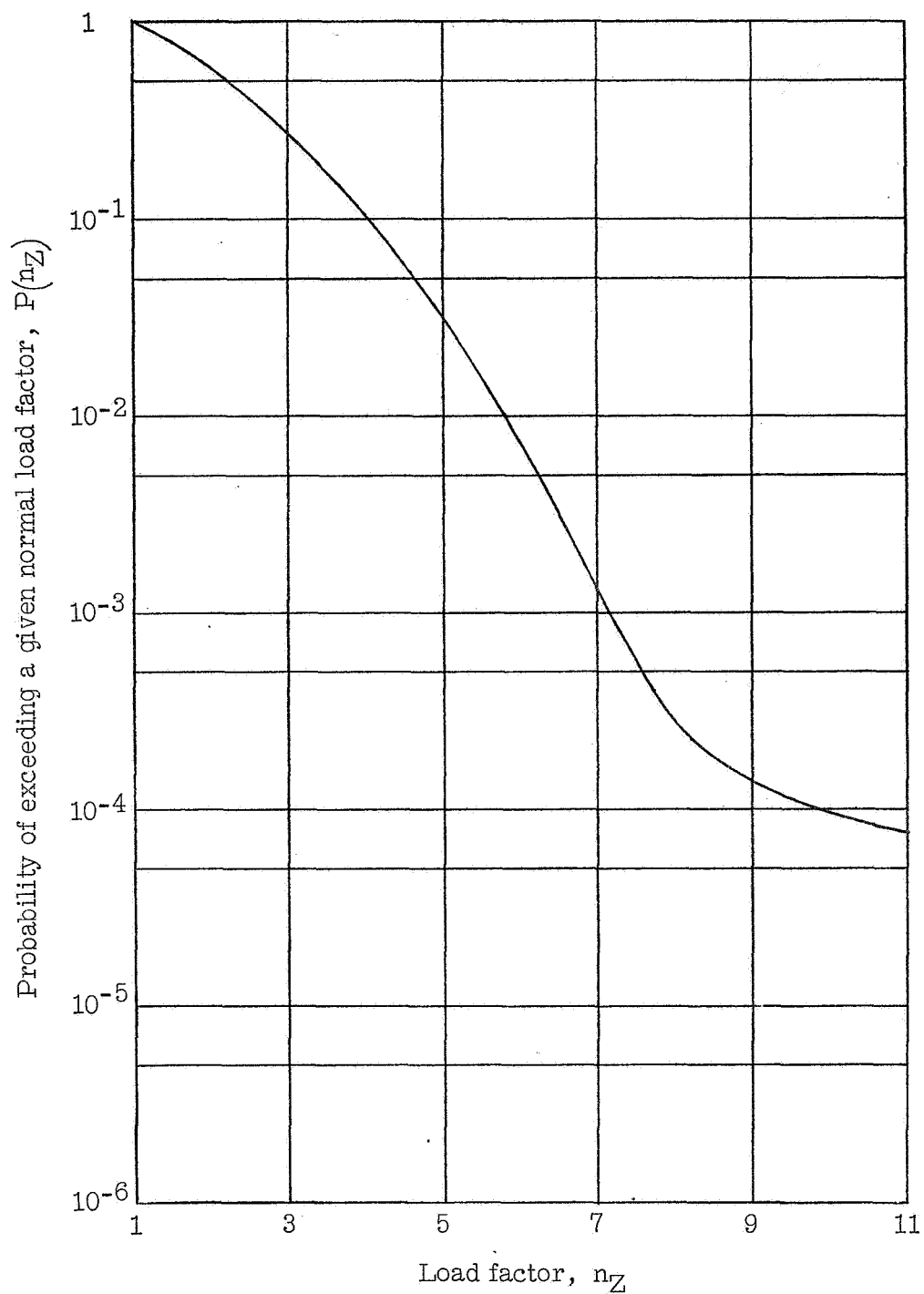


Figure 10.- Probability curve for wing load used in determining optimum limit horizontal- and vertical-tail loads in example problem.

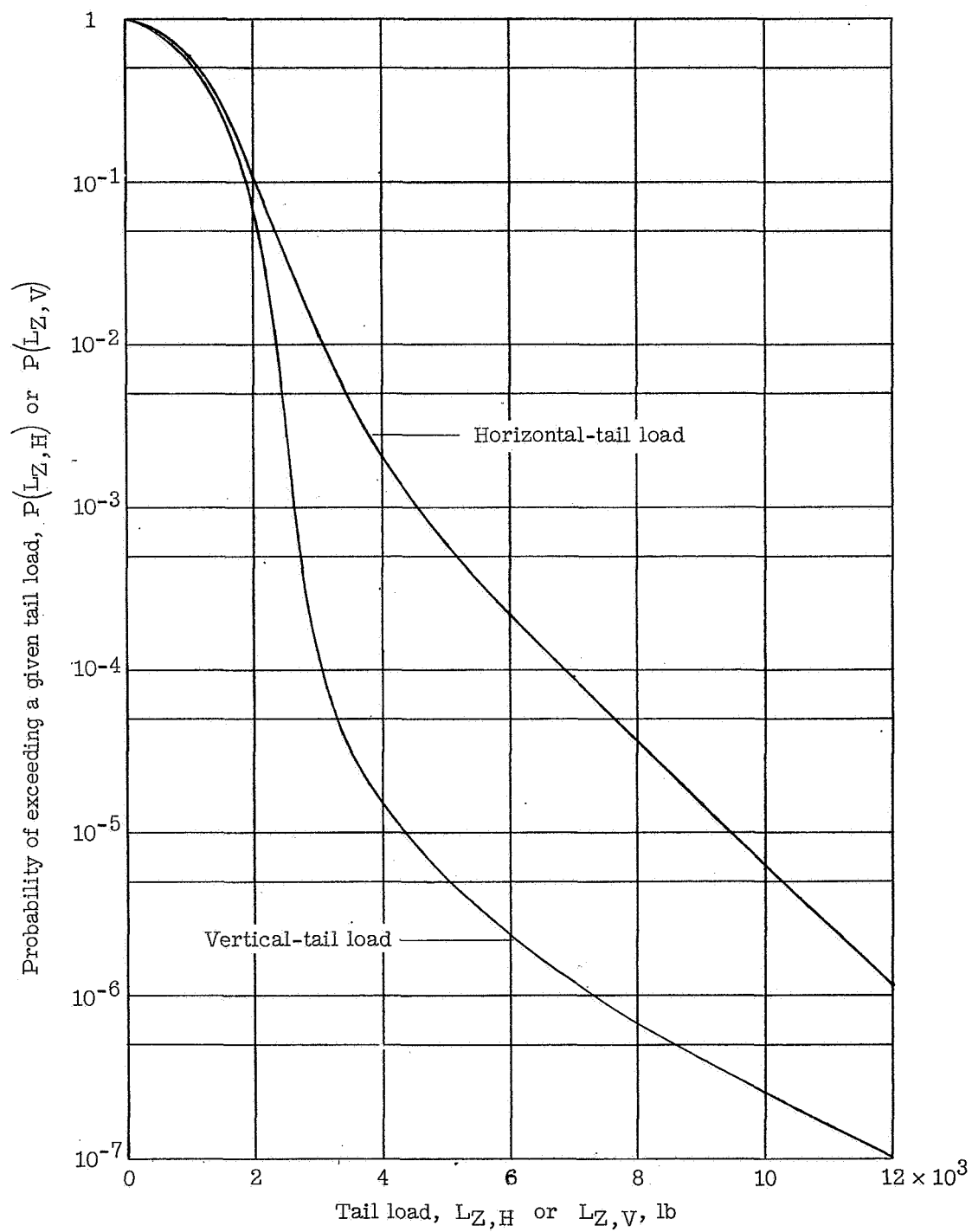


Figure 11.- Probability curves for tail loads used in determining optimum limit tail loads in example problem.

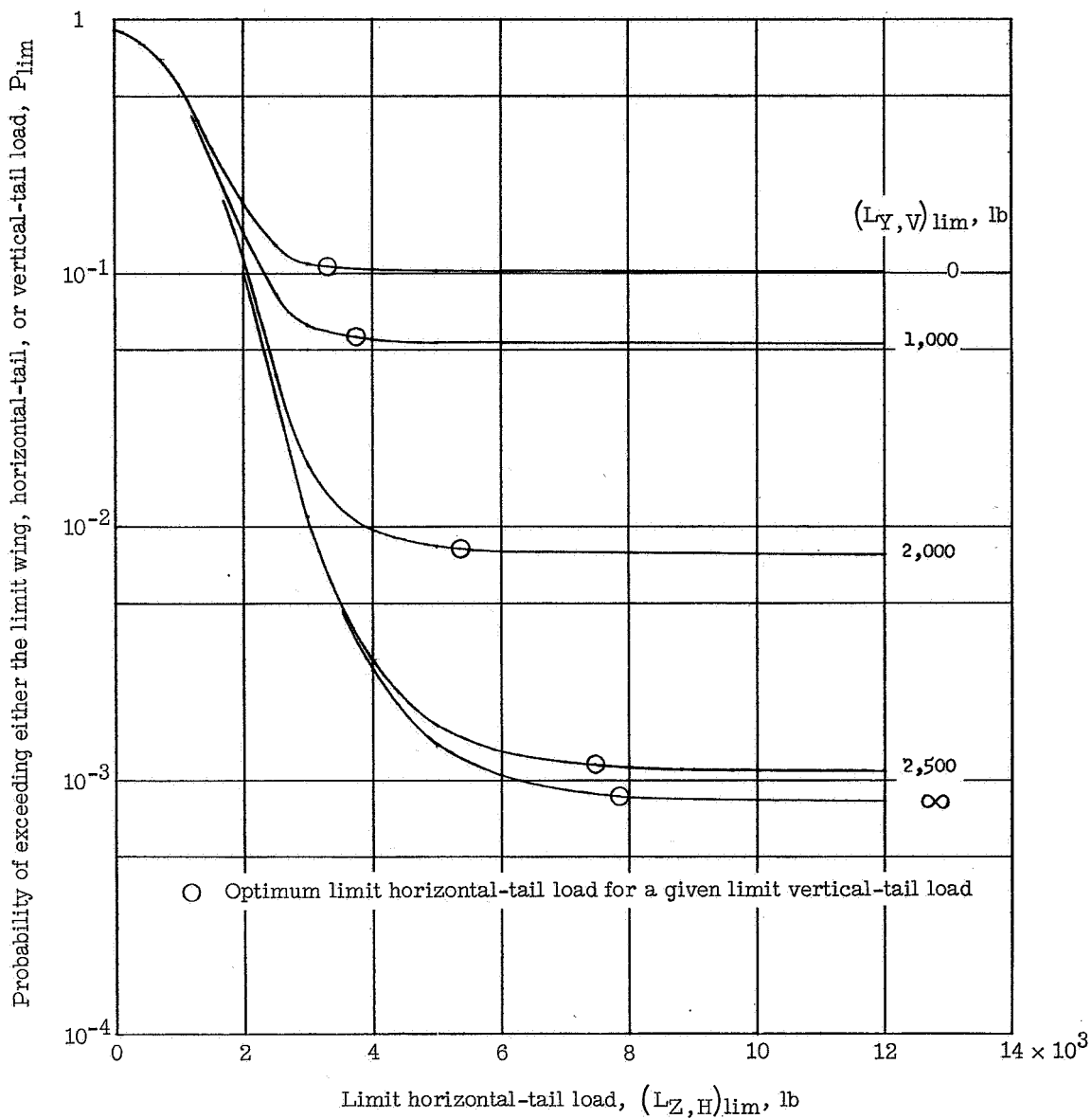


Figure 12.- Probability of exceeding either the limit wing load, the limit horizontal-tail load, or the limit vertical-tail load for given values of limit vertical-tail load.

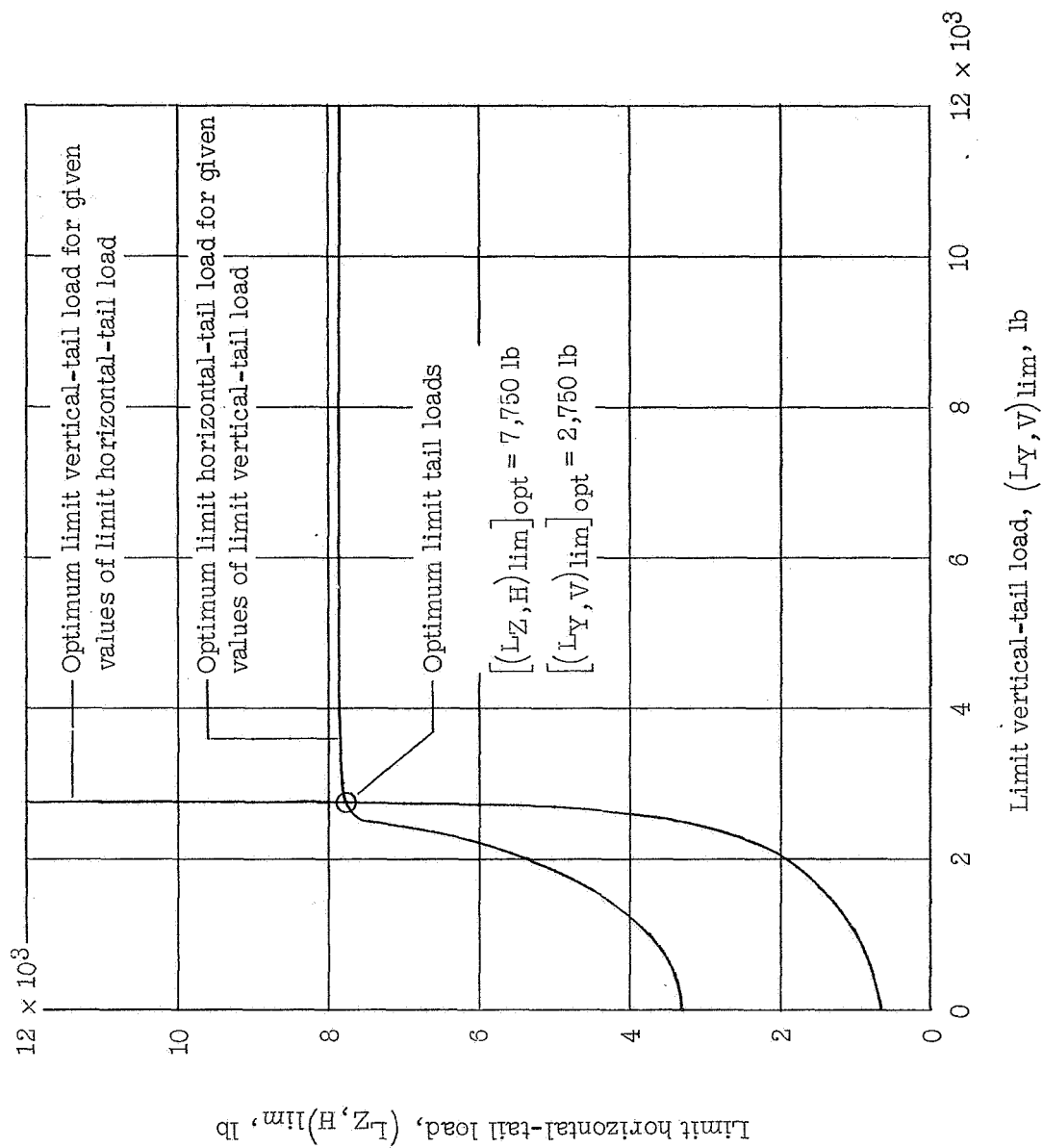


Figure 13.- Illustration of method of determining optimum limit tail loads.

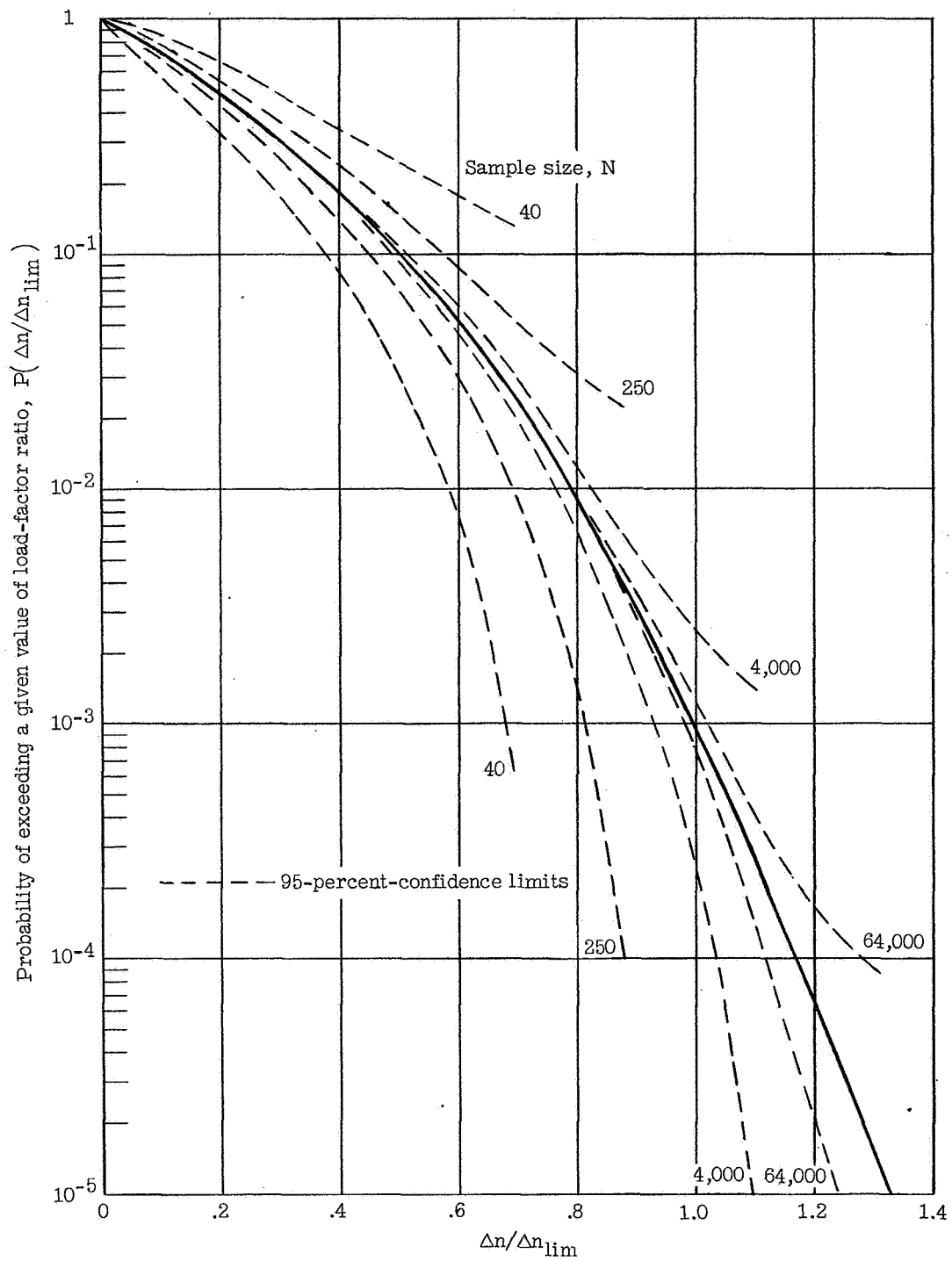


Figure 14.- Confidence curves for various sample sizes for a typical load factor probability curve.

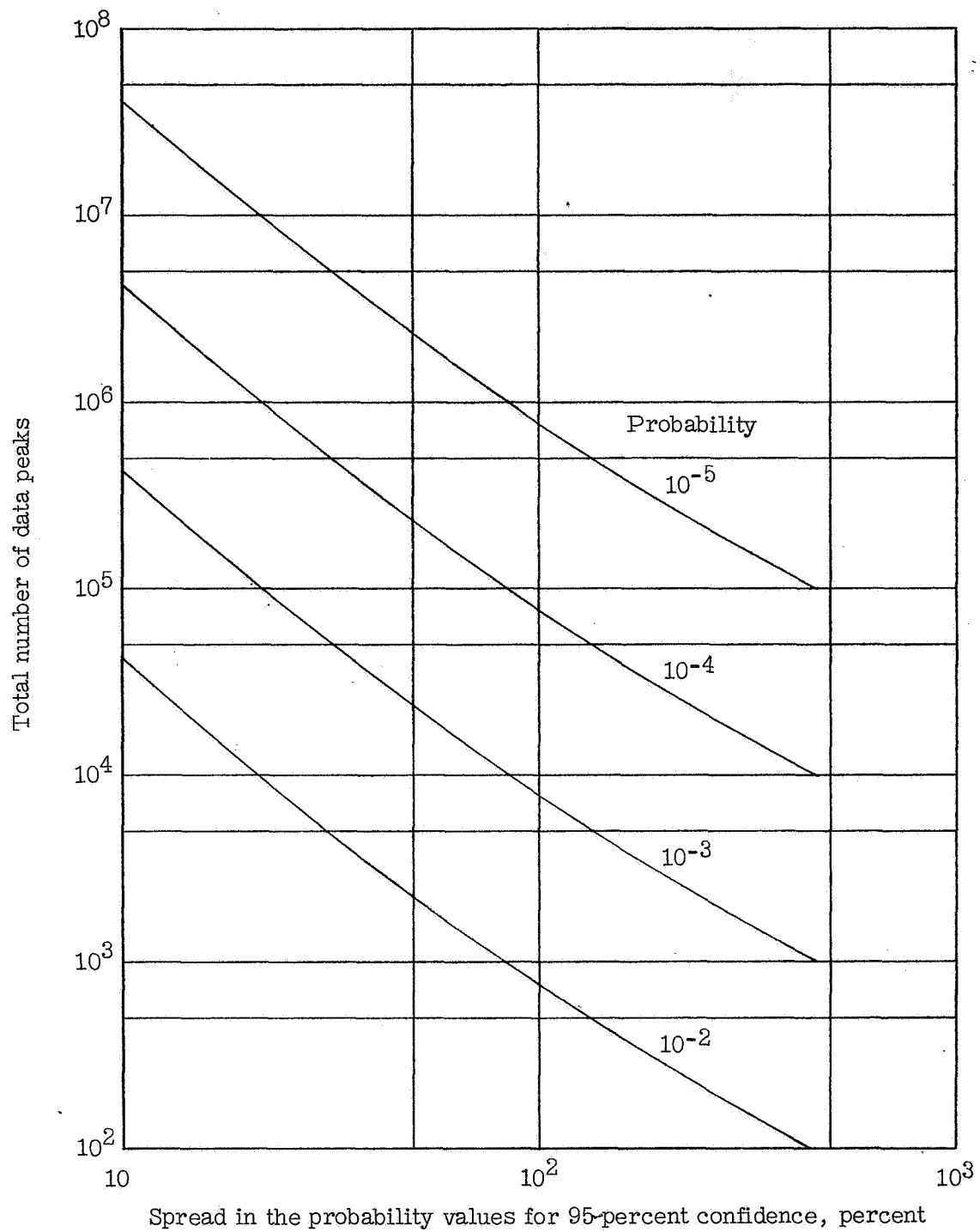
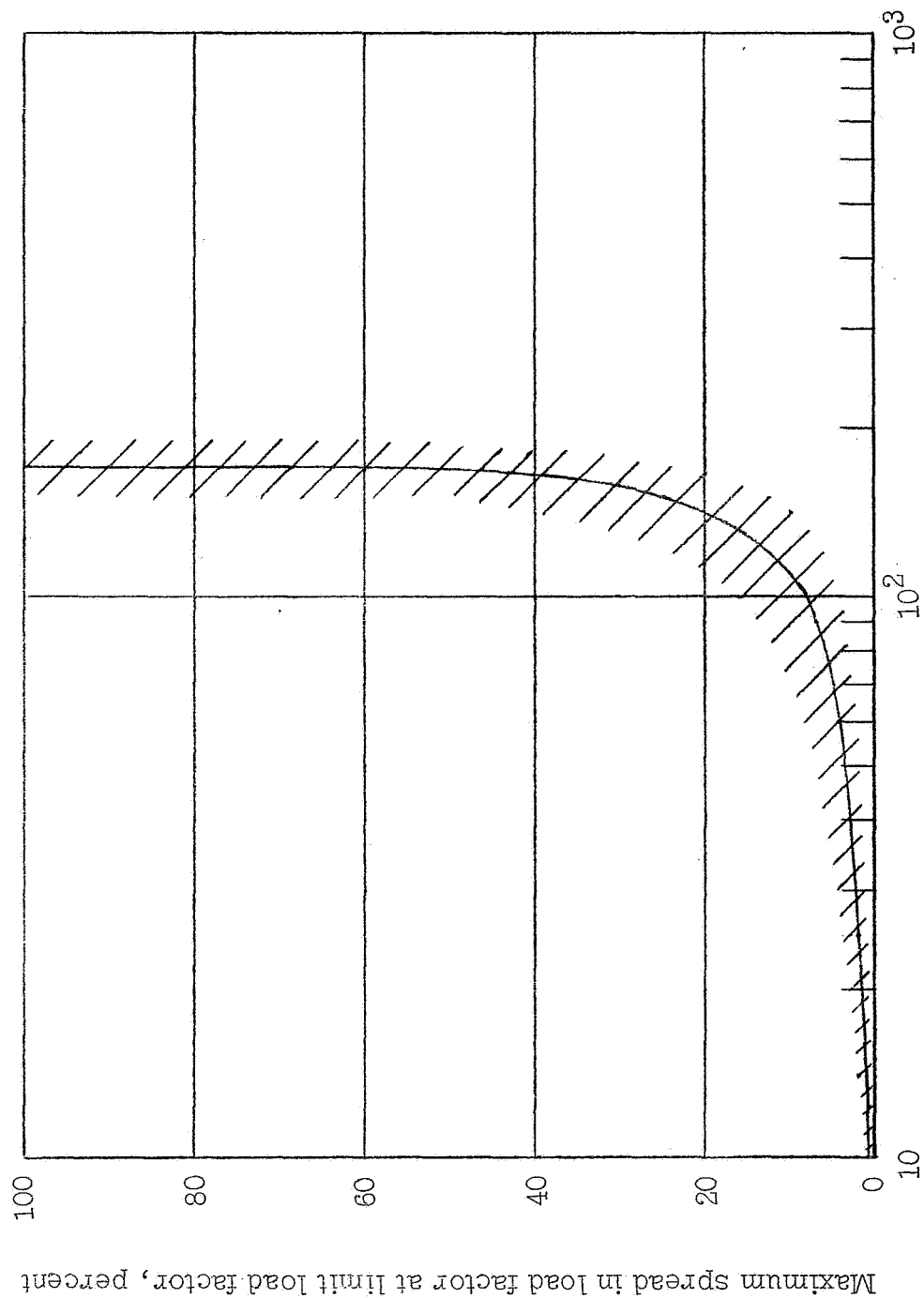


Figure 15.- Variation of the number of data peaks needed for a desired spread in the confidence interval at various probability levels.



Maximum spread in the probability values for 95 percent confidence, percent

Figure 16.- Variation of the maximum percent spread in load factor at limit load factor with the maximum percent spread in the probability values for 95-percent confidence limits.